

UNCLASSIFIED

AD NUMBER
AD451678
NEW LIMITATION CHANGE
TO Approved for public release, distribution unlimited
FROM Distribution authorized to DoD only; Administrative/Operational Use; Jun 1964. Other requests shall be referred to Director, US Army Tank-Automotive Center, Research and Engineering Dir., Warren, MI 48090.
AUTHORITY
USA TAC ltr, 10 Apr 1974

THIS PAGE IS UNCLASSIFIED

UNCLASSIFIED

AD 4 5 1 6 7 8L

DEFENSE DOCUMENTATION CENTER

FOR

SCIENTIFIC AND TECHNICAL INFORMATION

CAMERON STATION ALEXANDRIA, VIRGINIA



UNCLASSIFIED

NOTICE: When government or other drawings, specifications or other data are used for any purpose other than in connection with a definitely related government procurement operation, the U. S. Government thereby incurs no responsibility, nor any obligation whatsoever; and the fact that the Government may have formulated, furnished, or in any way supplied the said drawings, specifications, or other data is not to be regarded by implication or otherwise as in any manner licensing the holder or any other person or corporation, or conveying any rights or permission to manufacture, use or sell any patented invention that may in any way be related thereto.

451678L

CATALOGED BY DDC

AS AD No.

451678

SECURITY CLASSIFICATION: UNCLASSIFIED

COMPONENTS

R & D

LABORATORIES

LAND LOCOMOTION LABORATORY

Report No. 8524

LL No. 99

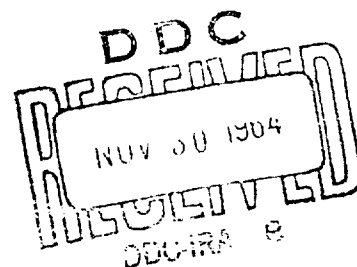
Copy No. 23

THE SHEAR TO NORMAL STRESS RELATIONSHIP
BETWEEN A RIGID WHEEL AND DRY SAND

By

Lt. Col. Aharon D. Sela

June 1964



Project No: 5016.11.84400

D/A Project No: 597-01-006

Authenticated:

Ronald A. Liston
RONALD A. LISTON
Chief, Land Locomotion
Laboratory
Components R&D
Laboratories

Approved:

John W. Wiss
JOHN W. WISS
Lt Colonel, Ordnance
Corps
Chief, Components R&D
Laboratories



U.S. ARMY TANK-AUTOMOTIVE CENTER
WARREN, MICHIGAN

SECURITY CLASSIFICATION: UNCLASSIFIED

REPRODUCED FROM
BEST AVAILABLE COPY

"THE FINDINGS OF THIS REPORT ARE NOT TO BE CONSTRUED AS AN OFFICIAL DEPARTMENT OF THE ARMY POSITION, UNLESS SO DESIGNATED BY OTHER AUTHORIZED DOCUMENTS."

DDC AVAILABILITY NOTICE

U. S. MILITARY AGENCIES MAY OBTAIN COPIES OF THIS REPORT DIRECTLY FROM DDC. OTHER QUALIFIED DDC USERS SHOULD REQUEST THROUGH DIRECTOR, RESEARCH AND ENGINEERING DIRECTORATE, ATAC, WARREN, MICHIGAN.

DESTROY THIS REPORT WHEN IT IS NO LONGER NEEDED. DO NOT RETURN IT TO THE ORIGINATOR.

NOTE

This report was written by Lt. Colonel A. D. Sela, Israeli Army, who spent a year at the Land Locomotion Laboratory. Since the Author had to comply with a definite deadline date set for his return, he tried to run as many experiments as possible before his departure from the U. S. A., with the intention of completing his analysis of the data upon his return to Israel. Therefore, the present report should not be regarded as a complete research paper. A full account of Colonel Sela's research will be published in the near future.

OBJECT

Study the shear stress distribution under a rigid wheel so that the mechanics of soil-tire interaction may be better understood and the flexibility of present prediction techniques enhanced.

RESULTS

The analytical method proposed in this report for the description of the shear and normal stresses as a function of contact angle, slip, wheel geometry, load and soil properties has been shown to be correct by means of experimental data obtained in sand.

CONCLUSIONS

Based on the analysis described in this report, it can be shown that in each soil there exists a particular load for a given wheel which allows the wheel to operate with maximum efficiency.

ADMINISTRATIVE INFORMATION

This program was supervised and conducted by the Land Locomotion Laboratory of ATAC under DA Project No. 1-A-0-13001-A-039, Project No. 5016.11.84400.

TABLE OF CONTENTS

	<u>Page No.</u>
Abstract	iii
Acknowledgement	iv
List of Symbols	v
List of Figures	vi
Introduction	1
Object	2
Summary	2
Conclusions	3
Recommendations	4
Theoretical Analysis	5
Distribution	21

ABSTRACT

Analytical expressions are formulated to describe the distribution of shear stresses which arise due to slip and soil flow.

The distribution of the shear and normal stresses along the wheel-soil interface is established as a function of slip. The stresses under a towed wheel are also described.

Actual measurements of the stresses by means of a special transducer embedded in the wheel are presented and compared to theoretical values. It is found that the agreement is satisfactory. It is concluded that further analysis of the available data will lead to a better understanding of the mechanics of tires operating off-the-road and to an improvement in wheeled vehicle prediction techniques.

ACKNOWLEDGEMENT

I wish to express my appreciation to all members of the Land Locomotion Laboratory who assisted me in the research that served as a basis for this paper. In particular, I mention Mr. R. A. Liston, Chief of the Laboratory, who arranged my visit to the laboratory; First Lieutenant Claude B. Parker who assisted in the conduct of my experimental program and made many valuable suggestions; and Mr. Marvin Jefsen, who assisted me in setting up my equipment, aided in its calibration and in the conduct of the tests. Without the assistance of the latter two individuals, I would not have been able to finish my work in a one year period.

LIST OF SYMBOLS

s	Shear Stress	(lbs./in. ²)
p	Normal Stress	(lbs./in. ²)
ϕ	Angle of Internal Friction	(°)
d	Soil Shear Displacement	(in.)
K	Tangent Modulus of Shear Curve	(in.)
d_i	Shear Displacement Due to Slip	(in.)
D	Wheel Diameter	(in.)
α_o	Contact Angle Measured from Bottom Dead Center (B.D.C.)	(Radians)
α	Central Angle of Point in Question from B.D.C.	(Radians)
i	Per Cent of Slip or Skid	Dimensionless
ΔA	Elementary Contact Area	(in. ²)
α_d	Critical Central Angle	(Radians)
d_f	Shear Displacement Due to Flow	(in.)
m	Coefficient of Proportionality between $\frac{D}{2} \times (\alpha - \alpha_o)$ and d_f	Dimensionless
α_r	Angle at which Shear Stresses Change their Sense	(Radians)
α_{r_o}	α_r for Zero Torque	(Radians)
β_o	Contact Angle to the Rear of B. D. C. . . .	(Radians)

LIST OF FIGURES

- Figure 1. Theoretical relation for shear and normal stresses (s/p) along the contact area of a rigid wheel operating in sand.
- Figure 2. Bulldozing and compacting zones at the wheel-soil interface.
- Figure 3A. Soil shear displacement expressed in degrees for various skid rates.
- Figure 3B. Ratio of shear and normal stresses as a function of the contact angle.
- Figure 4. General view of the test rig.
- Figure 5. Test wheel, Drive & Torque slip ring assembly.
- Figure 6. Load cell, showing cantilever to measure shear stresses and the thin beam on its top to measure normal pressure.
- Figure 7. The assembled load cell.
- Figure 8A. Load cell assembled in wheel well.
- Figure 8B. Load cell covered with diaphragm.
- Figure 9. Load cell completely assembled in wheel.
- Figure 10. Soil processing apparatus.
- Figure 11. Soil processing.
- Figure 11A. Tiller
- Figure 11B. Processing
- Figure 12. Leveling the processed soil.
- Figure 13. Soil bin ready for testing.
- Figure 14. Ruts made by the wheel, with various slip/skid rates, (wheel load of 50 pounds).
- Figure 14A. High slip rate.

- Figure 14B. High skid rate.
- Figure 14C. Low slip/skid rate.
- Figure 15. Experimental K values vs normal pressure.
- Figure 16. Experimental values of $\tan \phi$ versus normal pressure.
- Figure 17. Soil stresses, shear (s) and normal (p) under a driven rigid wheel in sand.
- Figure 18. Soil stresses, shear (s) and normal (p) under a driven, rigid wheel in sand.
- Figure 19. Soil stresses, shear (s) and normal (p) under a driven, rigid wheel in sand.
- Figure 20. Soil stresses, shear (s) and normal (p) under a driven, rigid wheel in sand.
- Figure 21. Soil stresses, shear (s) and normal (p) under a driven, rigid wheel in sand.
- Figure 22. Soil stresses, shear (s) and normal (p) under a driven, rigid wheel in sand.
- Figure 23. Soil stresses, shear (s) and normal (p) under a driven, rigid wheel in sand.
- Figure 24. Soil stresses, shear (s) and normal (p) under a driven, rigid wheel in sand.
- Figure 25. Soil stresses, shear (s) and normal (p) under driven, rigid wheel in sand.
- Figure 26A. Scatter of s/p for angles α_j along $\tan \alpha$ line.
- Figure 26B. Comparison between experimental and computed values of α_j .
- Figure 27. Soil stresses, shear (s) and normal (p) under a braked, rigid wheel in sand.
- Figure 28. Soil stresses, shear (s) and normal (p) under a braked, rigid wheel in sand.

- Figure 29. Soil stresses, shear (s) and normal (p) under a braked, rigid wheel in sand.
- Figure 30. Soil stresses, shear (s) and normal (p) under a braked, rigid wheel in sand.
- Figure 31. Soil stresses, shear (s) and normal (p) under a braked, rigid wheel in sand.
- Figure 32. Soil stresses, shear (s) and normal (p) under a braked, rigid wheel in sand.
- Figure 33. Soil stresses, shear (s) and normal (p) under a braked, rigid wheel in sand.
- Figure 34. Soil stresses, shear (s) and normal (p) under a braked, rigid wheel in sand.
- Figure 35. Soil stresses, shear (s) and normal (p) under a braked, rigid wheel in sand.
- Figure 36. Soil stresses, shear (s) and normal (p) under a braked, rigid wheel.
- Figure 37. Soil stresses, shear (s) and normal (p) under a braked, rigid wheel.
- Figure 38. Experimental vs computed values of $\frac{\alpha_o}{\alpha_r} - 1$ as a function of skid.
- Figure 39. A comparison between computed and experimental values of α_r , angle of shear stresses reversing point on braked wheels.
- Figure 40. Comparison of computed vs experimental values of α_{ro} .

I. INTRODUCTION

The mechanics of a pneumatic tire moving in soft soil is one of the most difficult and important basic problems in land locomotion research. Because of the extremely involved nature of the problem, a step by step method seems to be the only feasible avenue of approach for the solution. The first logical step is the investigation of the mechanics of a rigid wheel, because of the complications caused by the influence of the inflation pressure, the carcass stiffness and the tire tread are thus eliminated.

The mechanics of the rigid wheel-soft soil problem has been investigated by several researchers. (See Report No. 83.) In order to establish the basic equations of equilibrium various assumptions have been made concerning the pressure distribution along the soil-wheel interface surface. The actual measurement of pressures has been attempted first in 1960 by Vincent, Uffelman, and Hegedus. The conclusion of these studies was that the tangential stresses play a more important role than that had been assumed by previous investigators. Thus, the measurement of the tangential or sheer stresses along the wheel surface which had not been done in the past, was made to be the cornerstone of the present investigation. Uffelman measured tangential stresses, but he used a lug on the

wheel surface for this purpose, thus he altered the stress pattern under the wheel.

The author had established an analytical method for the description of the shear stress distribution prior to the beginning of the test series. The first analysis of the test data seems to support the aforementioned theoretical method.

II. OBJECT

The object of this study was to verify the author's theoretical work on the mechanics of a rigid wheel by means of experiments. The experimental apparatus allowed the measurement of all the factors influencing the equilibrium of the wheel including the tangential stress distribution. The program was expected to give a definite answer to some questions hitherto "avoided" by making unsupported assumptions. The final goal of this work, therefore, was to improve the understanding of the mechanics of a tire working off the road and hence to lead to the improvement of present wheeled vehicles design techniques as well as to provide better methods for wheel performance prediction.

III. SUMMARY

This study includes both theoretical and experimental investigation of the shear to normal pressure ratio distribution under a rigid wheel operating in sand. The

ability to predict this ratio is of great importance, since it will enable a designer to evaluate the influence of wheel dimensions on the performance of a wheel in a given soil. It has been found that the experimental results support the proposed theory with satisfactory accuracy.

IV. CONCLUSIONS

The following conclusions are drawn:

(a) At the leading portion of a wheel-soil interface the soil particles are pushed (bulldozed) forward, whereas along the trailing portion the soil is displaced rearward.

(b) A critical point on the interface, characterized by ϕ_d , separates the two zones. This point may be approximated by the theory presented in this report.

(c) In the case of a towed wheel, the bulldozing zone extends from bottom dead center to the leading edge of the interface.

(d) From the analysis and test results, one can show that there exists a given load for each soil and wheel under which the wheel operates with maximum efficiency. The computation of this load will be presented in a subsequent report.

V. RECOMMENDATIONS

Since this study is the first of its kind, it provides a basis for a preliminary understanding of the behavior of soil under a wheel. It also provides the basis for more extensive studies along the following lines:

1. The function of soil shear displacement due to soil flow.
2. A further study to investigate better wheel design.

A study of a rigid wheel on soft soils should be considered as the first part of a program which has as its second phase a study of pneumatic tires on a hard surface. Based on the results of the first two, a third and final phase should be devoted to the study of pneumatic tires on soft soil.

VI. THEORETICAL ANALYSIS

The Coulomb coefficient of friction in its broader meaning can, for soil, be used to describe the ratio of shear to normal stresses as a function of shear deformation. The ability of a wheel to develop traction, overcome soil resistance and the soil braking moment depends entirely upon the degree to which it mobilizes the shear forces along the interface of the wheel and the soil. It follows, then, that if one knows the shear-force deformation relationship of a soil and the shear deformation of each point along the wheel contact area, the ratio of shear to normal stresses can be predicted (1). Such an ability is of great importance since it will enable a designer to evaluate the influence of various wheel dimensions on the performance of a wheel in a given soil.

The theoretical analysis is based on two assumptions:

- 1 -That the shear stress-strain relationship of the soil is known and can be mathematically described;
- 2 -That the soil displacement associated with shear stresses can be analyzed by standard engineering methods and can also be mathematically described.

Shear displacement under the wheel is caused by a combination of slip or skid and soil flow. By introducing

displacement values obtained for points along the contact area into the stress-strain equation, the ratio of shear to normal stress is readily obtained. The mathematical description of the shear stress-strain relationship of a soil has been adequately presented in Ref. 1. Bevameter measurements indicate that this relationship can be expressed for sand by the general equation:

$$\frac{s}{p} = \tan \phi \left(1 - e^{-\frac{d}{k}}\right) \dots \dots \dots (1)$$

It has been shown (2) that the shear displacement due to slip or skid is proportional to the slip rate and the distance from the point in question to the leading edge of the contact area. The displacement for a rigid wheel in soil can be expressed mathematically as follows:

$$d_i = \frac{D}{2} (\alpha_o - \alpha) i \dots \dots \dots (2)$$

By neglecting soil displacement due to flow, the $\frac{s}{p}$ ratio along the contact area is described by introducing the value of 'd_i' from Equation (1) into Equation (2).

*Slip and skid are defined in this paper as follows:

$$\begin{aligned} \text{Slip} &= 1 - \frac{V}{V_t} \\ \text{Skid} &= 1 - \frac{V_t}{V_a} \end{aligned}$$

$$\frac{s}{p} = \tan \phi \left[1 - e^{-\frac{D}{2} k (\alpha_0 - \alpha) i} \right] \dots (3)$$

Figure 1 shows a family of curves where the $\frac{s}{p}$ ratio is plotted as a function of the contact angle, α , for various slip rates in a dry sand.

The flow of a soil particle under a wheel depends on the resultant force produced by the wheel on the particle. At any point under the wheel there exists a normal pressure, p , and a shear stress, s , which are defined in terms of forces as follows:

$$\text{Normal force } \Delta N = p \Delta A$$

$$\text{Shear force } \Delta S = s \Delta A$$

where,

ΔA is the contact area between the particle and the wheel. Since these forces are vectors, their horizontal components will be,

$$\Delta N_h = p \Delta A \sin \alpha$$

$$\Delta S_h = s \Delta A \cos \alpha$$

where,

$$V_a = \text{Linear velocity of the wheel}$$

$$V_t = \text{Tangential velocity of the wheel}$$

Although both slip and skid are denoted by positive values of i , the context in which ' i ' is used leaves little room for error concerning which of these values is being dealt with.

Figure 2 shows that the two horizontal components assume opposite directions in the case of a driven wheel. The soil particles will move in the direction of the resultant force since it is the difference of the two horizontal forces. Following this reasoning it can be seen that when $p \Delta A \sin \alpha > s \Delta A \cos \alpha$, the soil particle will be pushed forward and eventually be bulldozed out of the rut. If $p \Delta A \sin \alpha < s \Delta A \cos \alpha$, the soil particle will be displaced rearward and eventually embedded in the rut.

Under a slipping wheel, the leading portion of the contact area satisfies the first condition whereas the trailing portion satisfies the second. At the critical point on the soil-wheel interface, α_d , which divides the leading from the trailing portion, a condition occurs where $p \Delta A \sin \alpha_d = s \Delta A \cos \alpha_d$ or $\frac{s}{p} = \tan \alpha_d \dots (4)$

The leading portion of the contact area is usually associated with soil displacement by bulldozing, whereas the trailing portion is associated with compaction. The additional displacement by soil flow in the bulldozing zone obviously adds to the total shear displacements and hence affect the $\frac{s}{p}$ ratio. The intersection of the $\frac{s}{p}$ curve with the $\tan \alpha$ curve occurs at α_d . Values of α_d for various slip rates may be readily obtained from Figure 1.

The actual value of displacement due the soil flow is difficult to ascertain. If this value is assumed to be a linear function of the distance from α_d to the point in question, a mathematical model can be established to better understand what is happening in the bulldozing zone. Thus, the displacement due to flow is:

$$d_f = \frac{D}{2} (\alpha - \alpha_d) m \dots \dots \dots (5)$$

where m is the coefficient of proportionality. The $\frac{s}{p}$ ratio in the bulldozing zone is then obtained by introducing this value in Equation (1) as follows:

$$\frac{s}{p} = \tan \phi \left\{ 1 - e^{-\frac{D}{2K} [(\alpha_o - \alpha)i = (\alpha - \alpha_d)m]} \right\} \quad (6)$$

Values obtained for $\frac{s}{p}$ by Equation (6) at very low slip rates show that over a certain contact length $\frac{s}{p}$ is greater than $\tan \alpha$. Such a condition will require a reversal of the flow direction and hence is impossible. One might conclude from this that the rate of flow over this length of contact is not linear as previously assumed. It is felt that the rate of flow in this region diminishes to such values that the displacement keeps the $\frac{s}{p}$ ratio close to $\tan \alpha$. Flow in the leading portion approaches its full value as α approaches α_o . Experimental results for higher slip rates justify the assumption of a linear relation

for displacement as given in Equation 6. The curves describing $\frac{s}{p}$ for the bulldozing zone in Figure 1 have been constructed in light of the above considerations for slip conditions.

In the case of the skidding wheel, a towed wheel with braking moment, the horizontal components of normal and tangential forces are seen to act in the forward direction over the entire contact length. This implies that the bulldozing zone extends from bottom dead center to the forward leading edge, α_0 , or that $\alpha_d = 0$. Experimental data indicate that shear stresses due to skid reverse direction. This implies also that the relative shear displacement between the wheel and the soil reverses its direction at a point α_r along the contact area. The total shear displacement at each point under the wheel will be the absolute value of the difference of shear displacements due to skid and flow or:

$$d_t = \frac{D}{2} \left| \left[(\alpha_0 - \alpha) i - \alpha_m \right] \right| \dots \dots \dots (7)$$

This displacement and the related $\frac{s}{p}$ curves are described in Figure 3 for various skid rates.

Equation 7 indicates that at some points along the contact area the shear stress is zero when the condition $(\alpha_0 - \alpha) i = m \alpha$ is satisfied. In solving for this

critical location, defined as α_r , we find:

$$\alpha_r = \frac{\alpha_o}{1 + \frac{m}{i_o}} \dots \dots \dots (8)$$

In the forward direction from α_r the shear stress is positive while to the rear the sign becomes negative. Analysis of Equation 8 shows that as the skid approaches zero, α_r also approaches zero. In such a case the shear stresses along the entire contact area are positive and a driving moment must be applied to balance these stresses.

By assuming a symmetrical negative and positive shear stress distribution, an assumption justified by experimental evidence at conditions of zero torque, α_r will be located in the center of the contact area as follows:

$$\alpha_{r_o} = \frac{\alpha_o - \beta_o}{2} \dots \dots \dots (9)$$

A simultaneous solution of Equations 8 and 9 yield the rate of skid for these conditions:

$$\frac{\alpha_o - \beta_o}{2} = \frac{\alpha_o}{1 + \frac{m}{i_o}}$$

$$i_o = m \cdot \frac{\alpha_o - \beta_o}{\alpha_o + \beta_o} \dots \dots \dots (10)$$

Figure 3 is plotted for the case in which,

$$i_o = (.30) \left(\frac{50 - 10}{50 + 10} \right) = .20$$

This analysis shows that a simply towed wheel is a particular case of a braked wheel where the braking moment is equal to zero. Further reflection indicates that the torque produced by the negative shear stresses balances both the applied braking torque T_b and the braking torque produced by the positive shear stresses under the wheel.

$$\frac{D}{2} \int_{\beta_0}^{\alpha_r} s dA = T_b + \frac{D}{2} \int_{\alpha_r}^{\alpha_0} s dA$$

In the condition where $T_b = 0$, we find:

$$\int_{\beta_0}^{\alpha_r} s dA = \int_{\alpha_r}^{\alpha_0} s dA$$

The practical significance of a braked wheel is largely confined to agricultural needs where the tow force applied to the vehicle frame is also utilized to operate some implement. However, a towed wheel ($T_b = 0$) is of considerable importance to the military. The analysis of the skidding wheel was included in this study to provide as complete a description as possible.

TEST EQUIPMENT

Figures 4 to 14 illustrate the test equipment and the soil bin used for this study. The dimensions of the bin are approximately 20 feet long by 5 feet wide and

filled with about 14 inches of loose dry sand. The width of the bin permitted three separate passes of the wheel without lateral disturbance between passes as shown in Figure 13. The soil was processed to a depth of 10 inches by a tiller that rotates about a vertical axis, and then leveled by a leveling board mounted on the dynamometer carriage. The complete processing cycle is illustrated in Figures 10 to 12.

The test equipment for this study was designed to measure the following parameters: sinkage, torque, angular wheel position, linear carriage position, drawbar-pull, shear, and normal stresses along the wheel-soil interface. A series of tests were run with vertical loads of 50, 100, 150, 200, 250 and 300 pounds applied by means of dead weights. For each load the conditions of slip and skid were varied from 0 to approximately 100%. The test parameters were recorded simultaneously on a six-channel recorder which also had an event marker.

The measurement of each parameter involved difficulties which could provide the theme of a separate paper. The simplest measurement was the sinkage. This was obtained with a linear potentiometer mounted on the dynamometer carriage and referenced from the soil surface.

Torque was measured by a torque gage located on one

side of the wheel on the wheel axles between the wheel and the gear train.

Drawbar-pull was measured with a strain gaged cantilever mounted on the other side of the wheel. The cantilever measured the force transferred from the wheel to the carriage.

Figures 5 to 9 illustrates the transducers used to measure shear and normal stresses. In essence, the shear stress was measured by a strain gaged cantilever located as an integral part of the normal stress transducer on the periphery of the wheel. The transducer's electronic signal was transferred from the wheel to the recorder through slip rings.

The rate of slip and skid as defined on Page 4 is a comparison of the distance traveled by the periphery of the wheel to that traveled by the carriage (or wheel axle) during the same increment of time.

These distance values were recorded simultaneously as a function of time on the recorder in 5° increments for the wheel periphery and for a corresponding distance of axle travel. A microswitch and event marker were used to indicate when the shear and normal transducers were at bottom dead center of the wheel.

By varying the drive controls of the carriage and

wheel the various conditions of slip and skid were obtained. Braking moments were applied through a specially constructed unit in the gear train.

All transducers were calibrated using dead weights for loads and by means of direct measurements for linear readings. A special calibration technique was required for the drawbar-pull measurements to account for the effects of the driving or braking torque applied to the wheel. This influence is of importance in a device in which torque is supplied on one side of the wheel and the drawbar-pull measured on the other. A detailed analysis of this calibration technique is not considered appropriate in this paper. However, a note of warning is offered to caution the reader to consider any "coupling" between drawbar-pull and torque when dealing with the usual wheel dynamometer.

TEST RESULTS AND EVALUATION

The shear displacement parameters of the soil were determined by a Bevameter for various normal pressure values in order to compare the test results with the theoretical analysis. Figures 15 and 16 show the various values of K , the soil shear constant and $\tan \phi$, where ϕ is the angle of internal friction. Mean experimental values of $K = 1.0$ inch and $\tan \phi = .44$ ($\phi \approx 24^\circ$) were used in this study.

By introducing these values in Equation (1), we have:

$$\frac{s}{p} = .44 (1 - e^{-d})$$

The $\frac{s}{p}$ ratio may be readily computed theoretically for each point along the contact area by substituting 'd' in Equation (2) and Equation (5) for slip, and in Equation (7) for the skidding condition. This technique has been applied to the case of a driven wheel in Figures 17 through 25, where the plots of the upper portion of the graphs show experimental results of shear and normal stresses while the lower plots show a comparison of the experimental $\frac{s}{p}$ ratio with the computed values.

It can be seen that the general shape of the experimental and computed curves are qualitatively the same. Both of the curves climb to the left and right from a cusp point. It can be seen that the cusp points of the experimental curves are very close to the $\tan \alpha$ curve as could be expected. This shows that different shear displacement functions act to the left and to the right of the $\tan \alpha$ curve which is in agreement with the theoretical analysis. The theoretical conclusion that the $\frac{s}{p}$ ratio at α_d equals $\tan \alpha_d$ is verified. Hence α_d is seen to define the limits of the bulldozing and compacting zones.

Figure 26 shows a rather small scatter for a plot of experimental $\frac{s}{p}$ values obtained at the cusp points versus

$\tan \alpha_d$. Generally it is seen that lower slip values yield smaller values of α_d which is also in agreement with the theory.

Despite the good qualitative agreement in some cases, the expected quantitative disagreement requires some explanation. This disagreement is believed to occur due to a number of reasons:

1. The soil conditions are not homogeneous.
2. The soil flow in a direction transverse to wheel motion was not considered in the theoretical analysis. Since the shear transducer measures components in the longitudinal direction only, any flow to the side will mean that a stress value smaller than the true resultant causing the tangential and transverse flow will be sensed. This of course, implies equality in stress and strain directions which may not be true.

3. The soil displacement under the wheel may deviate from the linear relationship assumed.

4. Readings of the shear and normal stresses at both extremes of the contact area are low and thus a small error in reading causes a large error in the $\frac{s}{p}$ value.

In spite of the small quantitative deviations of the computed $\frac{s}{p}$ ratios from the experimental ratios, it is believed that the theoretical analysis satisfactorily describes the behavior of the soil-wheel system for a driven wheel.

For the braked wheel, the experimental results of shear and normal stresses at the wheel-soil interface are presented in Figures 27 through 37. A comparison between the computed and experimental values of $\frac{s}{p}$ is given in these curves. The major obstacle, however, arose due to the fact that the 'm' value in Equation (7),

$$d_t = \frac{D}{2} \left| \left[(\alpha_o - \alpha) i - \alpha_m \right] \right|$$

was difficult to define either theoretically as a function or as a constant. A few trial and error attempts have been made with fair success toward this end.

The first trial was to determine a constant value for 'm' by Equation (8):

$$\alpha_r = \frac{\alpha_o}{1 + \frac{m}{i}}$$

or:
$$\frac{\alpha_o}{\alpha_r} - 1 = \frac{m}{i}$$

Figure 38 shows a plot of $\log \frac{\alpha_o}{\alpha_r} - 1$ versus \log skid, i , and yields a constant value of $m = .65$. By using this value of 'm', Figure 39, which is a comparison between the experimental and computed values of α_r , could be constructed. In spite of the fact that there is a close correlation in this plot, the theory had to be discarded because if 'm' were of a constant value of 0.65, the skid rate would have to be over 55% for conditions of zero braking. This, in fact, does not occur. Figures 30, 31,

32 and 33 seem to indicate that the shear stresses obtained with an 'm' of .65 are too high to be acceptable.

The second approach to define 'm' was through the condition in which the wheel was towed at almost zero braking torque. Experimental evidence for this condition shows:

$$\alpha_{r_0} = \frac{\alpha_o - \beta_o}{2} \dots \dots \dots (9)$$

where, α_{r_0} is the point of shear stress reversal on the contact area for zero braking torque. It is assumed that 'm' remains constant at various slip rates and may be defined for zero torque by substituting α_{r_0} for α_r in Equation (8) or:

$$m = \frac{\alpha_o + \beta_o}{\alpha_o - \beta_o} i_o \dots \dots \dots (10)$$

Figure 40 shows a plot of α_{r_0} computed by Equation (9) versus experimental values of α_{r_0} . The agreement as seen in the plot is reasonably good, yet in order to define 'm' by utilizing this theory, a way must be found to define, theoretically, the rate of skid, i_o , for zero torque. It is felt that this may be achieved, but the data available from this set of experiments is inconclusive for this purpose.

As in the case of a driven wheel, it is thought that qualitatively good agreement for the skid condition exists

between theoretical and experimental results. In spite of the fact that the behavior of 'm' has not been established, it seems that a fundamental understanding of the skidding wheel-soil relationship has been achieved.

TECHNICAL REPORT DISTRIBUTION LIST

Title: The Shear To Normal Stress Relationship
Between A Rigid Wheel And Dry Sand

Report No.
8524

<u>Address</u>	<u>Copies</u>
Director, Research and Engineering Directorate (SMOTA-R)	1
Components Research and Development Laboratories	
ATTN: Administrative Branch (SMOTA-RCA)	2
Components Research and Development Laboratories	
ATTN: Materials Laboratory (SMOTA-RCM)	1
Systems Requirements and Concept Division	
ATTN: Systems Simulations Branch (SMOTA-RRC).	1
ATTN: Systems Concept Branch (SMOTA-RRD)	1
ATTN: Economic Engineering Study Branch (SMOTA-RRE)	1
ATTN: Systems Requirements Branch (SMOTA-RRF)	1
ATTN: Foreign Technology Section (SMOTA-RTS.2).	1
ATTN: Technical Information Section (SMOTA-RTS)	2
Commanding General	
U. S. Army Mobility Command	
ATTN: AMSMO-RR	1
ATTN: AMSMO-RDC	1
ATTN: AMSMO-RDO	1
Warren, Michigan 48090	
USACDC Liaison Office (SMOTA-LCDC)	2
Sheridan Project Office (AMCPM-SH-D)	1
U. S. Naval Civil Engineering	
Research and Engineering Laboratory	
Construction Battalion Center	
Port Hueneme, California	1
Commanding Officer	
Yuma Proving Ground	
Yuma, Arizona 85364	1
Harry Diamond Laboratories	
Technical Reports Group	
Washington, D. C. 20025	1

<u>Address</u>	<u>No. of Copies</u>
Defense Documentation Center Cameron Station ATTN: TIPCA Alexandria, Virginia 22314	20
Commanding General Aberdeen Proving Ground ATTN: Technical Library Maryland 21005	2
Commanding General Hq, U. S. Army Materiel Command ATTN: AMCOR (TW).	1
ATTN: AMCOR (TB).	1
Department of the Army Washington, D. C. 20025	
Land Locomotion Laboratory	2
Propulsion Systems Laboratory	5
Fire Power Laboratory.	1
Track and Suspension Laboratory	6
Commanding General U. S. Army Mobility Command ATTN: AMCPM-M60 Warren, Michigan 48090.	3
Commanding General Headquarters USARAL APO 949 ATTN: ARAOD Seattle, Washington	2
Commanding General U. S. Army Aviation School Office of the Librarian ATTN: AASPI-L Fort Rucker, Alabama	1
Plans Officer (Psychologist) PP&A Div, G3, Hqs, USACDCEC Fort Ord, California, 93941.	1
Commanding General Hq, U. S. Army Materiel Command Research Division ATTN: Research and Development Directorate Washington, D. C. 20025	1

<u>Address</u>	<u>No. of Copies</u>
Commandant Ordnance School Aberdeen Proving Ground, Md.	1
British Joint Service Mission Ministry of Supply P. O. Box 680 Benjamin Franklin Station ATTN: Reports Officer Washington, D. C.	2
Canadian Army Staff 2450 Massachusetts Avenue Washington, D. C.	4
British Joint Service Mission Ministry of Supply Staff 1800 K Street, N. W. Washington, D. C.	6
Director Waterways Experiment Station Vicksburg, Mississippi	3
Unit X Documents Expediting Project Library of Congress Washington, D. C. Stop 303	4
Exchange and Gift Division Library of Congress Washington, D. C. 20025.	1
Headquarters Ordnance Weapons Command Research & Development Division Rock Island, Illinois Attn: ORDOW-TB.	2
Army Tank-Automotive Center Canadian Liaison Office, SMOTA-LCAN.	4
United States Navy Industrial College of the Armed Forces Washington, D. C. Attn: Vice Deputy Commandant	10
Continental Army Command Fort Monroe, Virginia	1

<u>Address</u>	<u>No. of Copies</u>
Dept. of National Defense Dr. N. W. Morton Scientific Advisor Chief of General Staff Army Headquarters Ottawa, Ontario, Canada	1
Commanding Officer Office of Ordnance Research Box CM, Duke Station Durham, North Carolina	3
Chief Office of Naval Research Washington, D. C.	1
Superintendent U. S. Military Academy West Point, New York Attn: Prof. of Ordnance	1
Superintendent U. S. Naval Academy Annapolis, Md.	1
Chief, Research Office Mechanical Engineering Division Quartermaster Research & Engineering Command Natick, Massachusetts	1

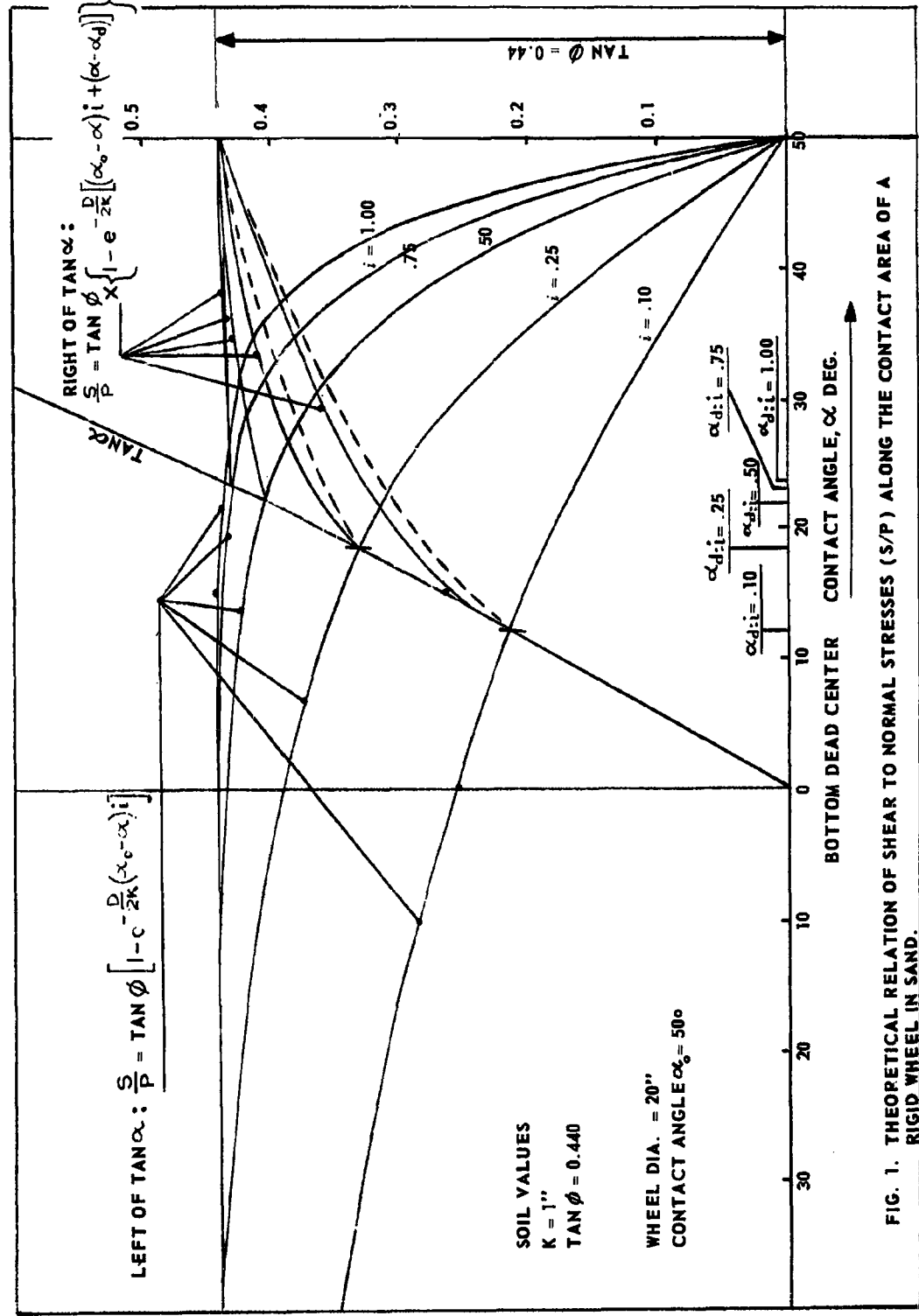


FIG. 1. THEORETICAL RELATION OF SHEAR TO NORMAL STRESSES (S/P) ALONG THE CONTACT AREA OF A RIGID WHEEL IN SAND.

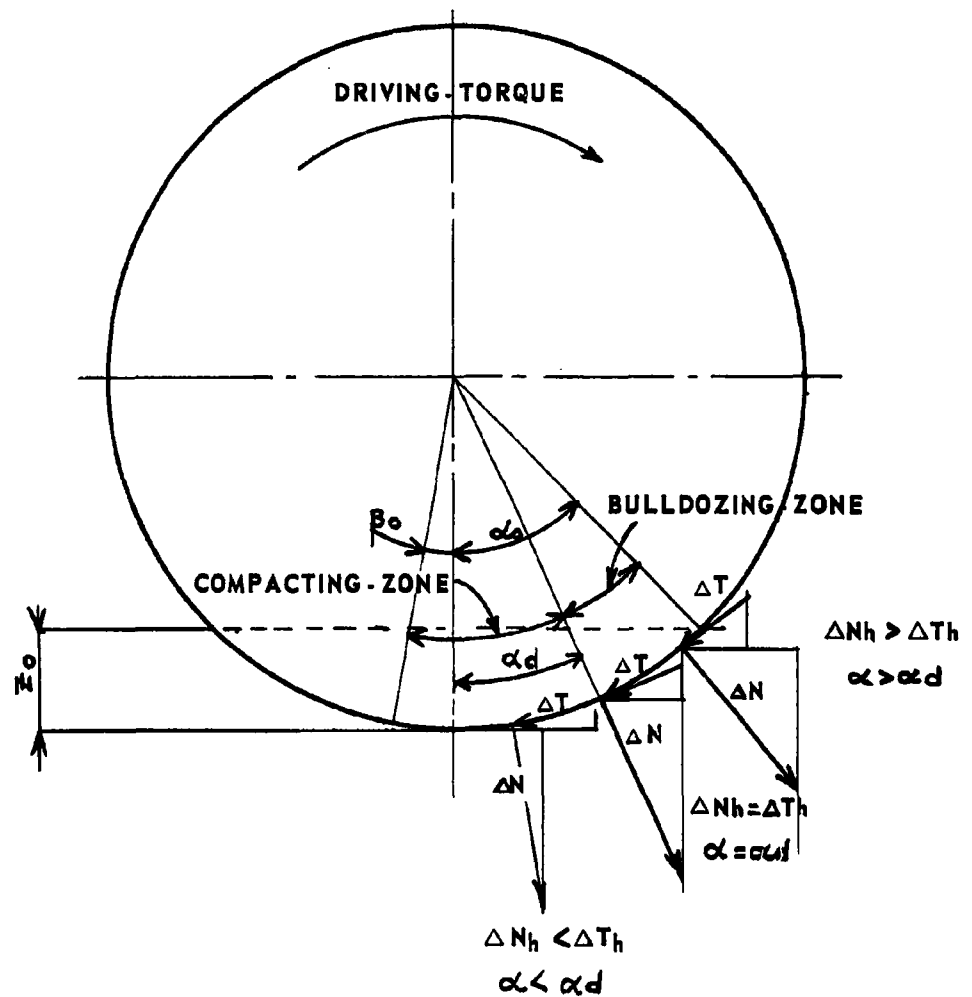


FIG. 2. BULLDOZING AND COMPACTING ZONES AT THE WHEEL - SOIL INTERFACE.

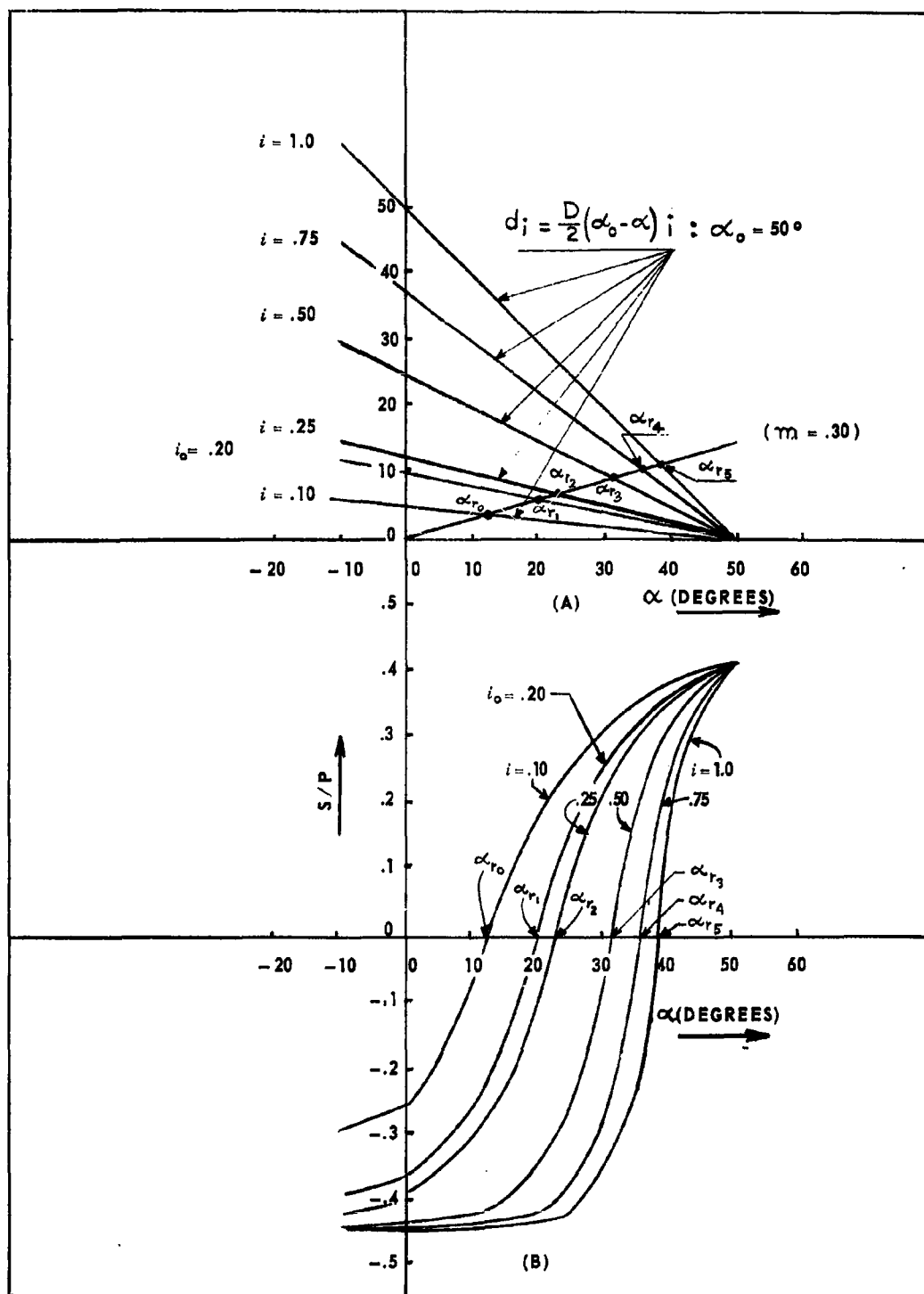


FIG. 3. A. SOIL SHEAR DISPLACEMENT, EXPRESSED IN DEGREES FOR VARIOUS SKID RATES.

B. S/P VS α FOR VARIOUS SKID RATES.

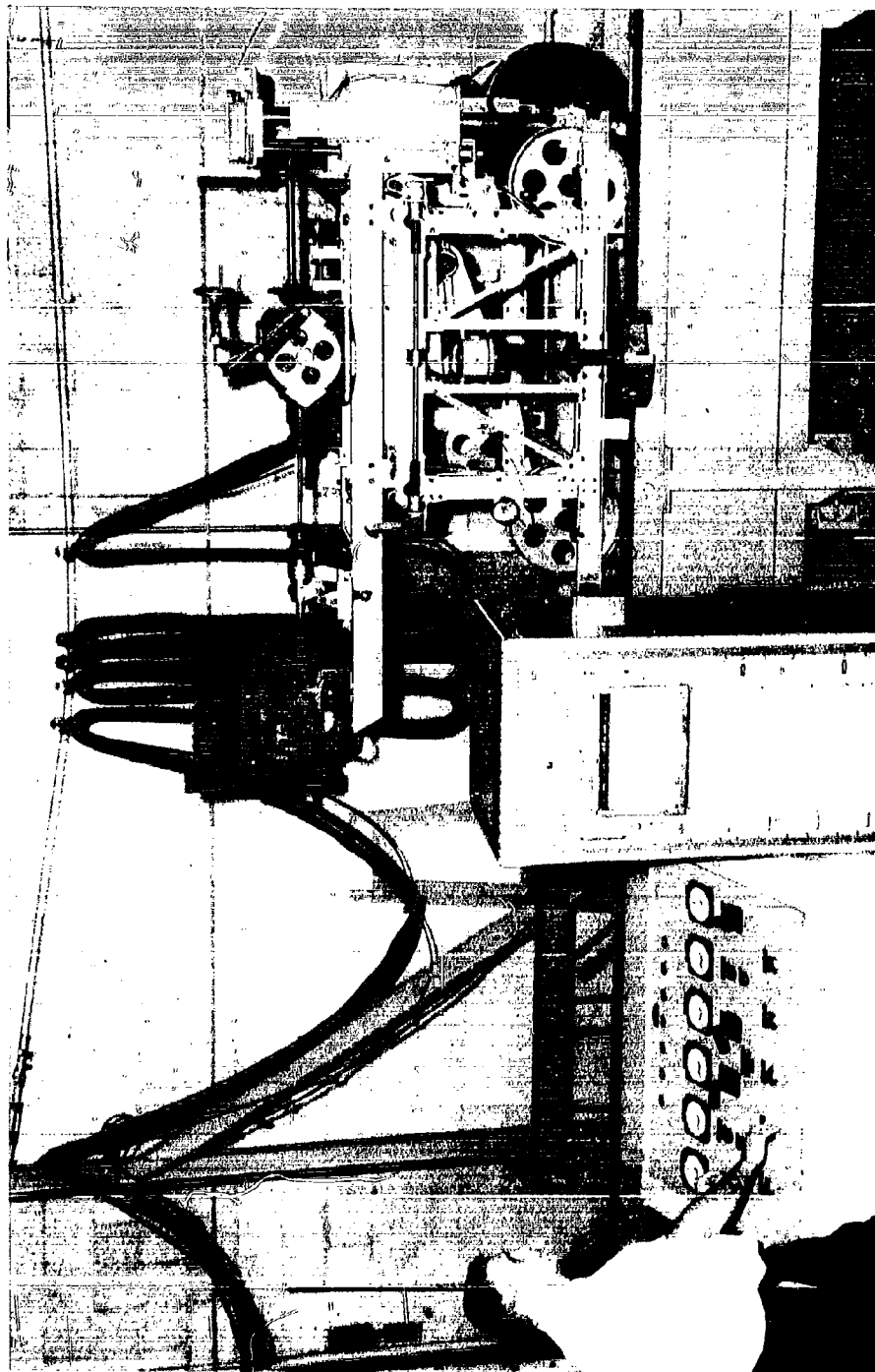


FIG. 4. GENERAL VIEW OF THE TEST RIG.

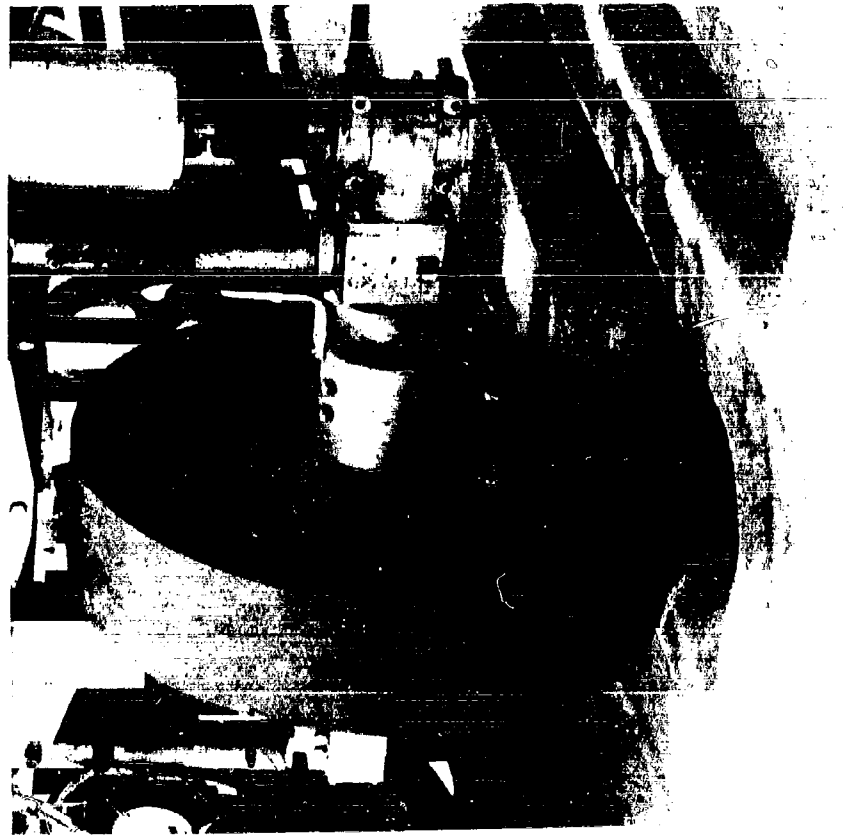


FIG. 5. TEST WHEEL, DRIVE AND TORQUE SLIP RING ASSEMBLY.

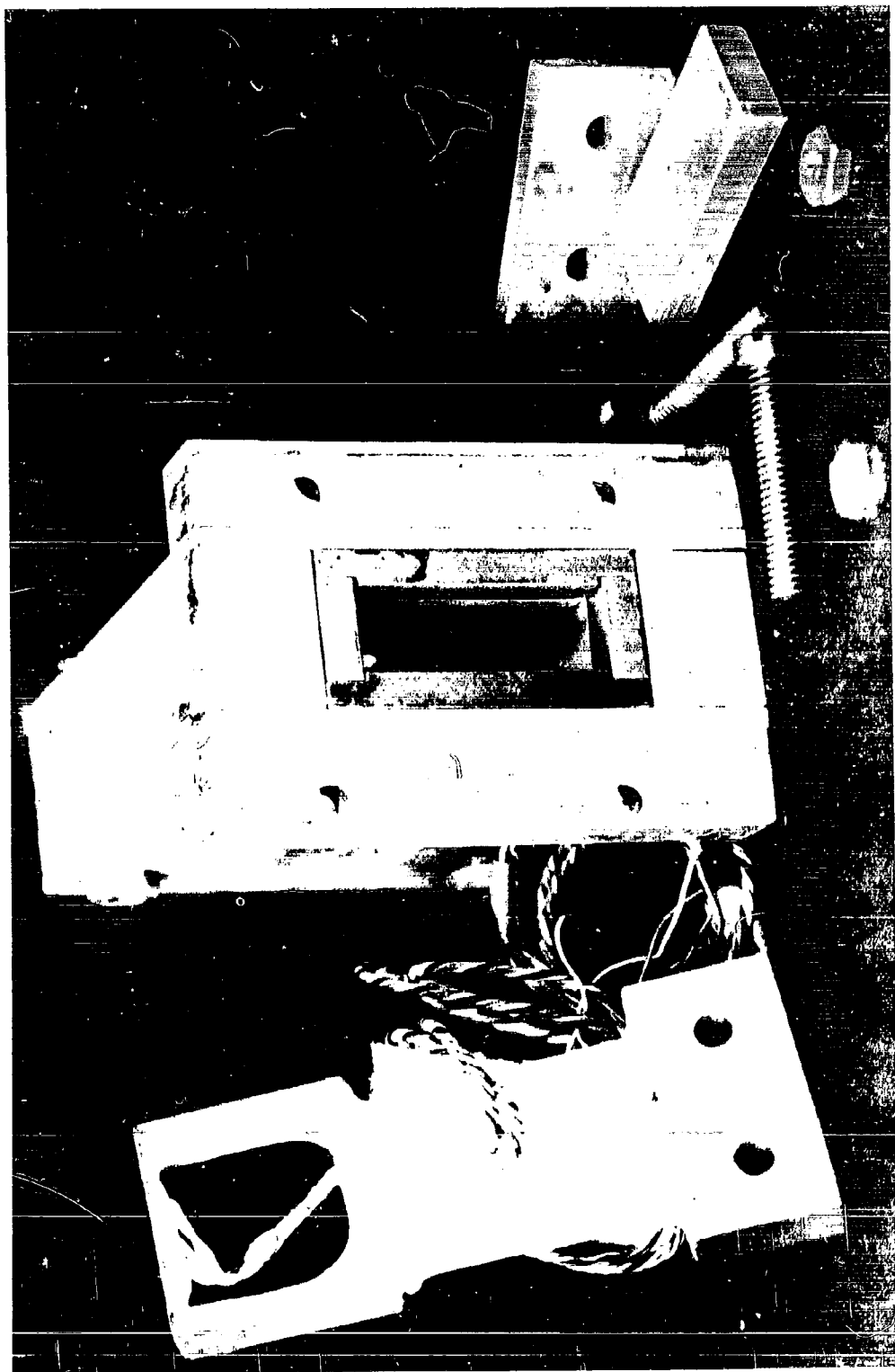
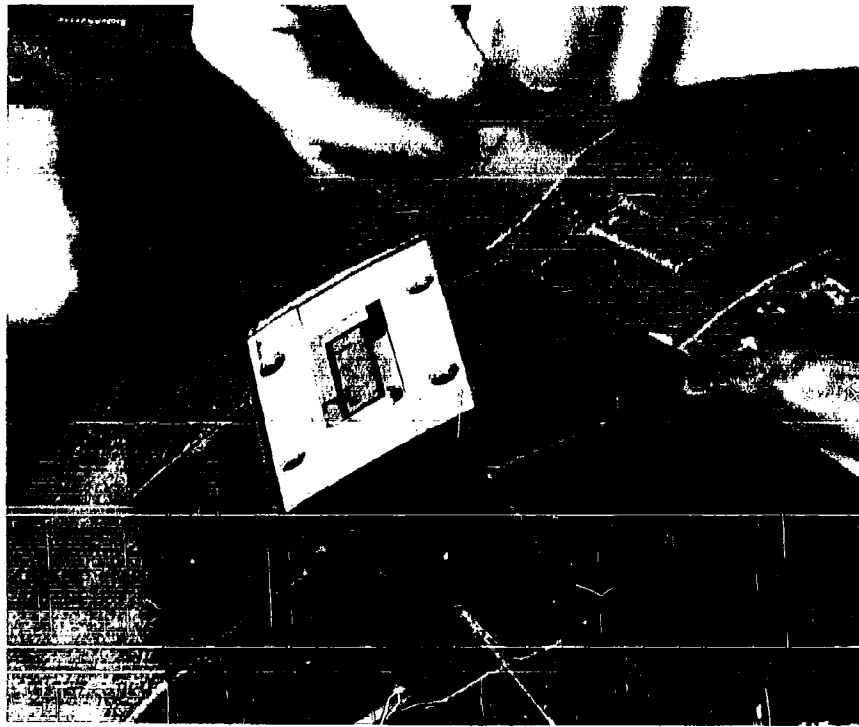


FIG. 6. LOAD CELL, SHOWING CANTILEVER TO MEASURE SHEAR STRESSES AND
THE THIN BEAM ON ITS TOP TO MEASURE NORMAL PRESSURE.



FIG. 7. THE ASSEMBLED LOAD CELL.



A. LOAD CELL ASSEMBLED IN WHEEL WELL.



B. LOAD CELL COVERED WITH DIAPHRAGM.

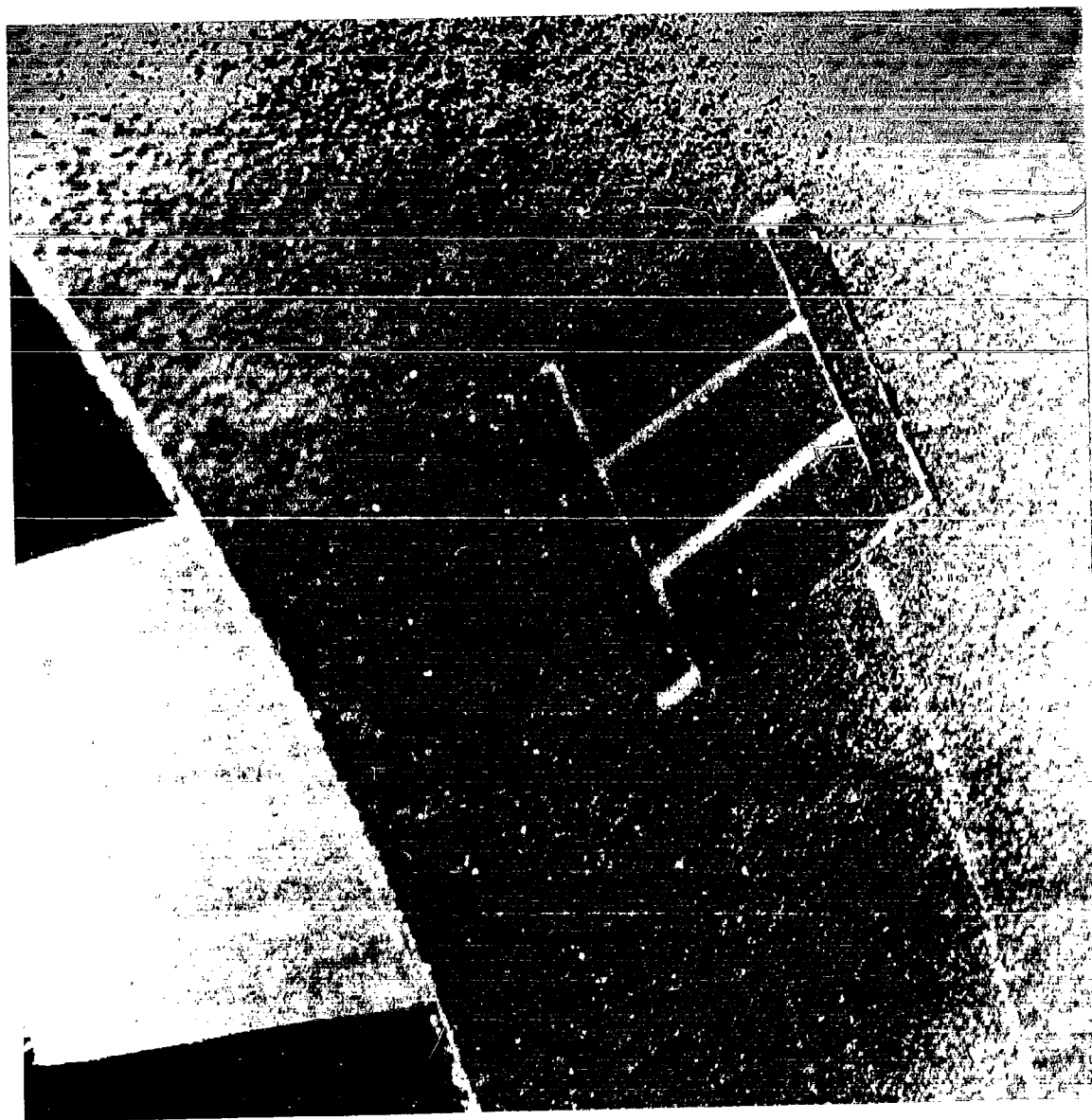


FIG. 9. LOAD CELL COMPLETELY ASSEMBLED IN WHEEL.

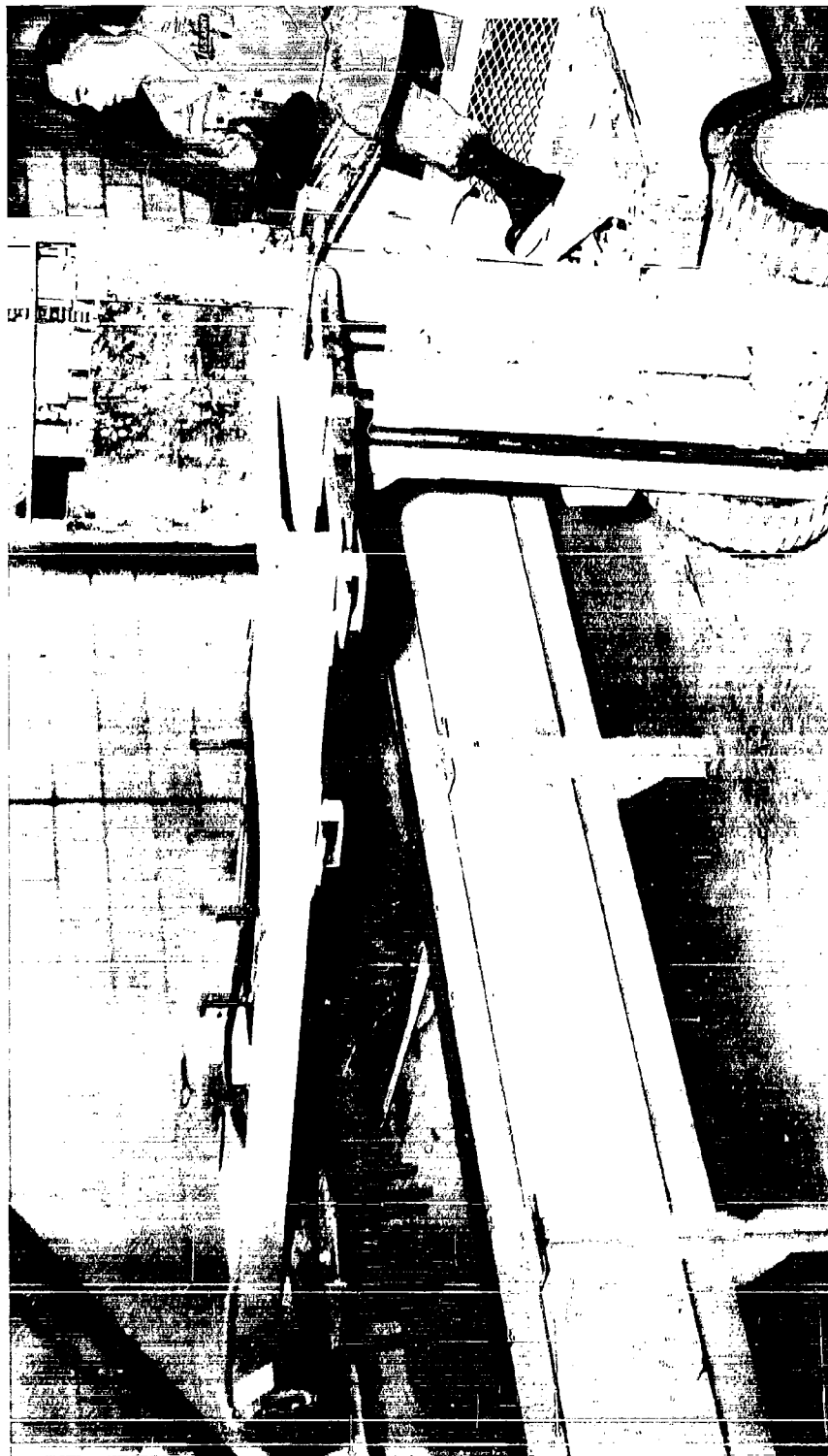
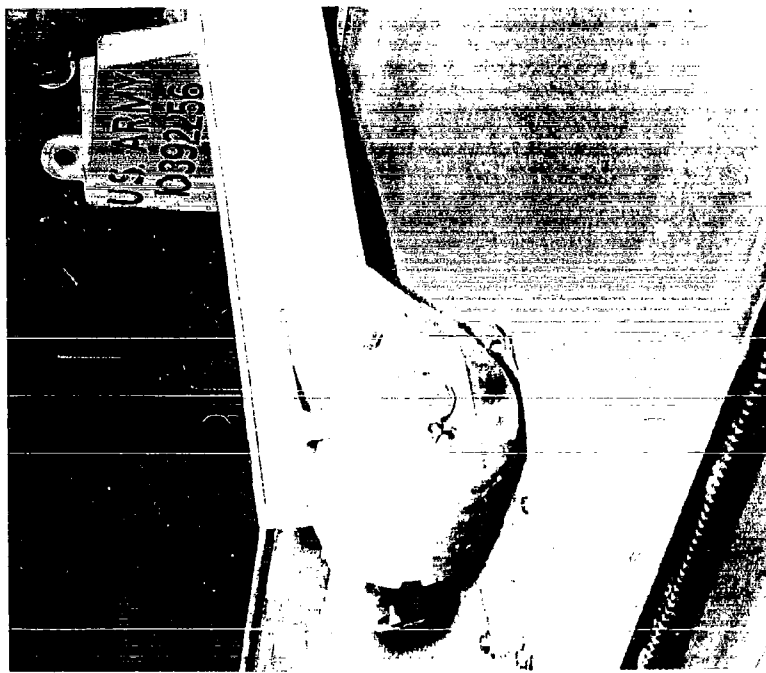


FIG. 10. SOIL PROCESSING APPARATUS.



A. TILLER.



B. PROCESSING.

FIG. 11. SOIL PROCESSING.

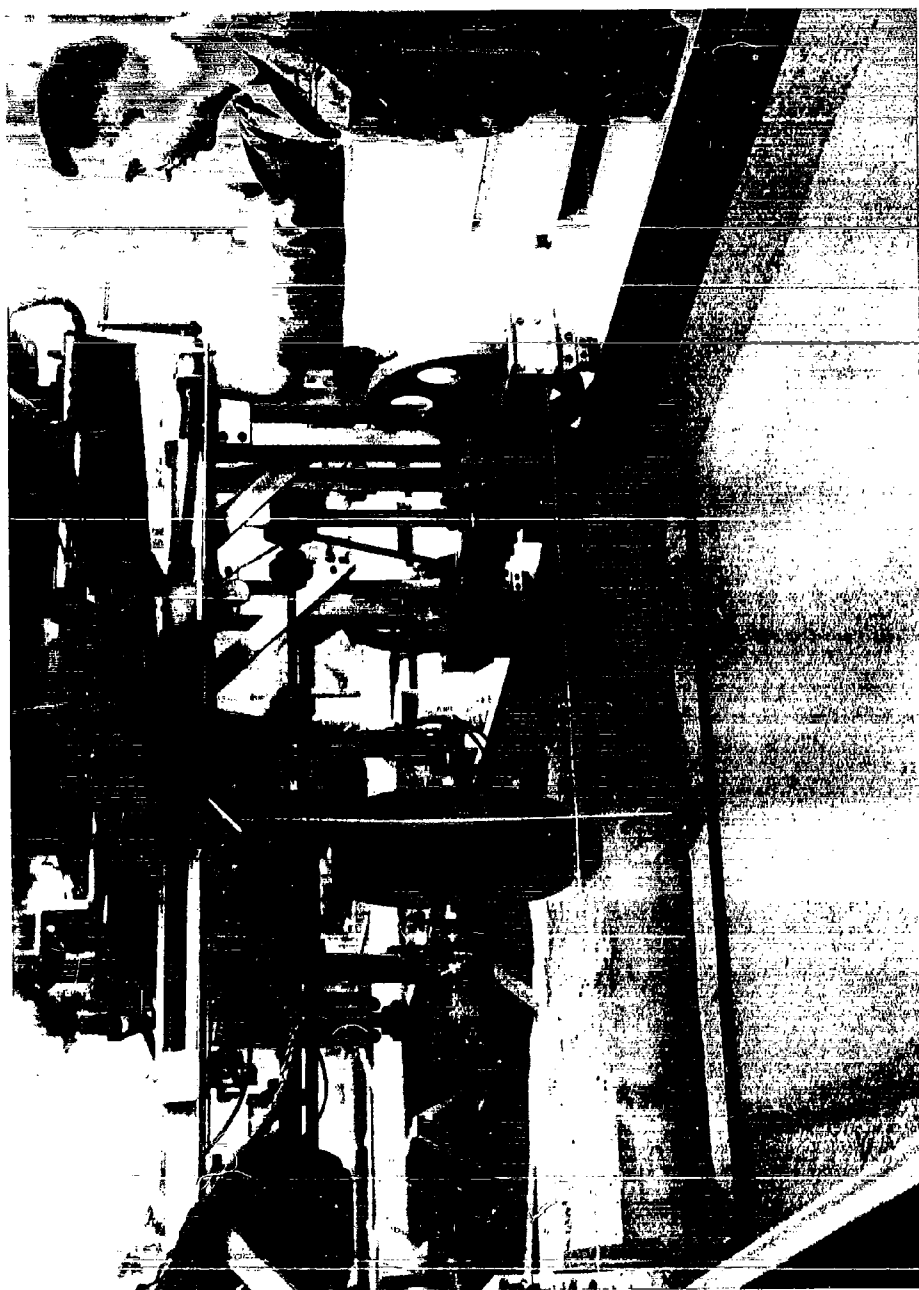


FIG. 12. LEVELING THE PROCESSED SOIL.

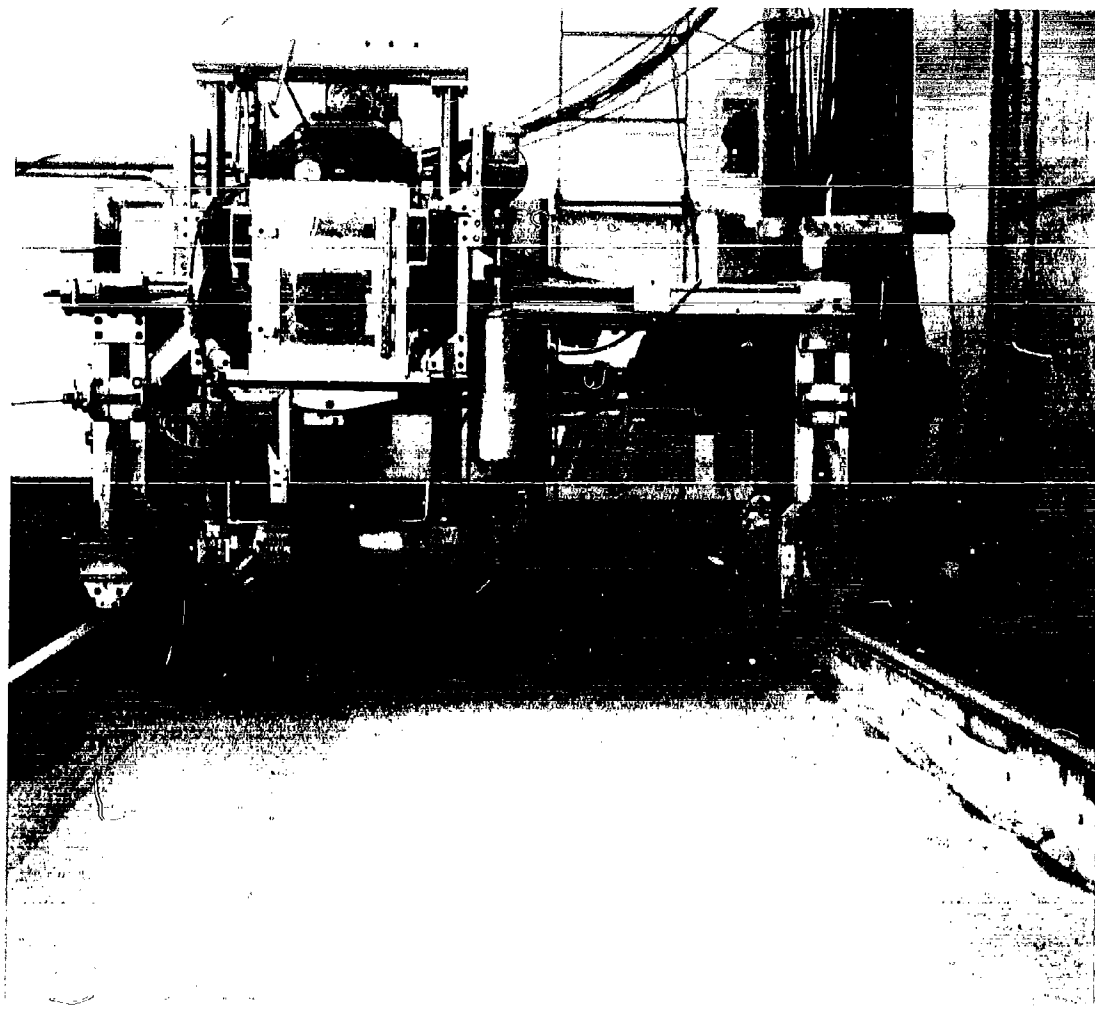


FIG. 13. SOIL BIN READY FOR TESTING.



A. HIGH SLIP RATE

B. HIGH SKID RATE.

C. LOW SLIP/SKID RATE

FIG. 14. RUTS MADE BY THE WHEEL, WITH VARIOUS SLIP/SKID RATES, (WHEEL LOAD OF 50 POUNDS).

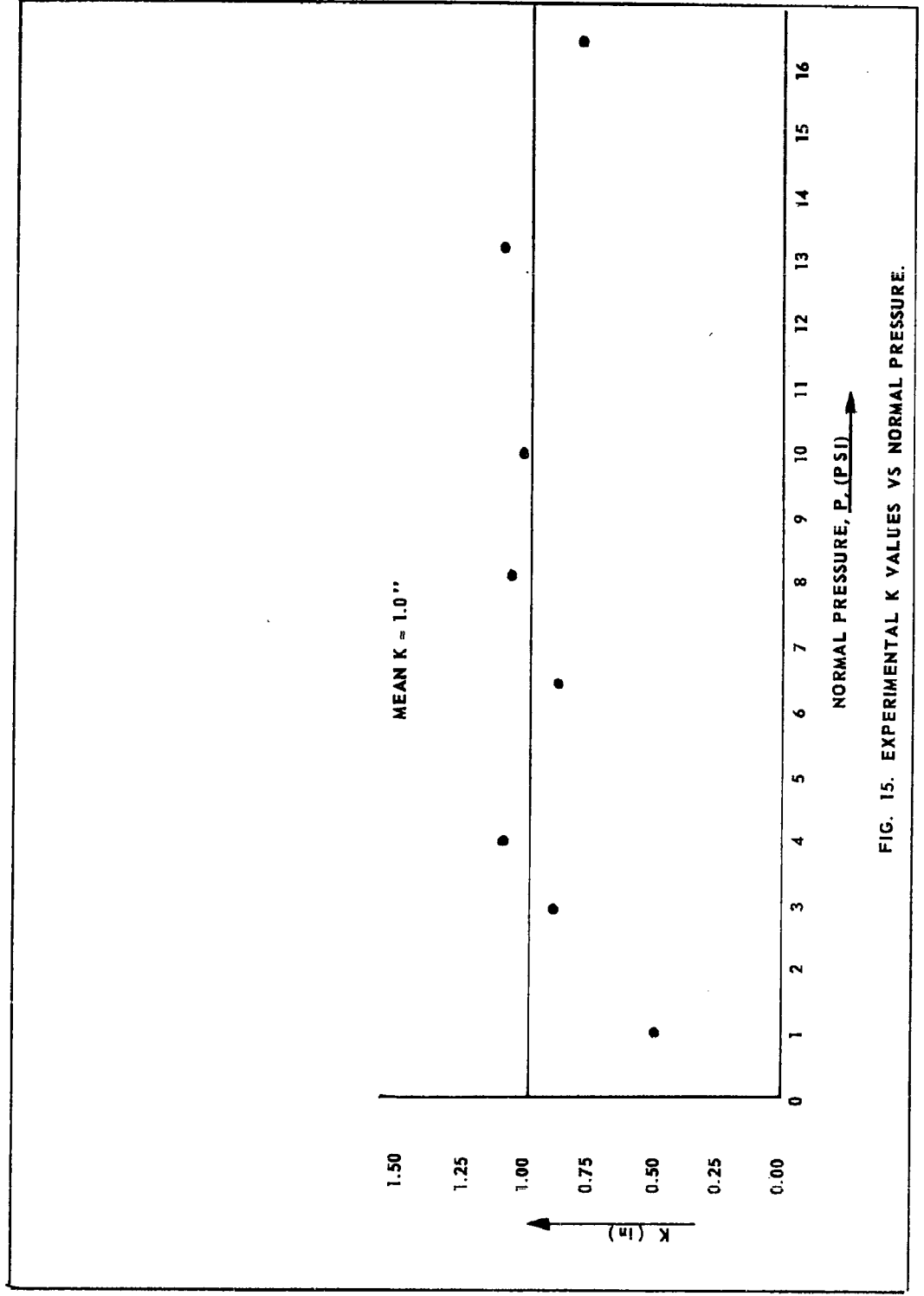


FIG. 15. EXPERIMENTAL K VALUES VS NORMAL PRESSURE.

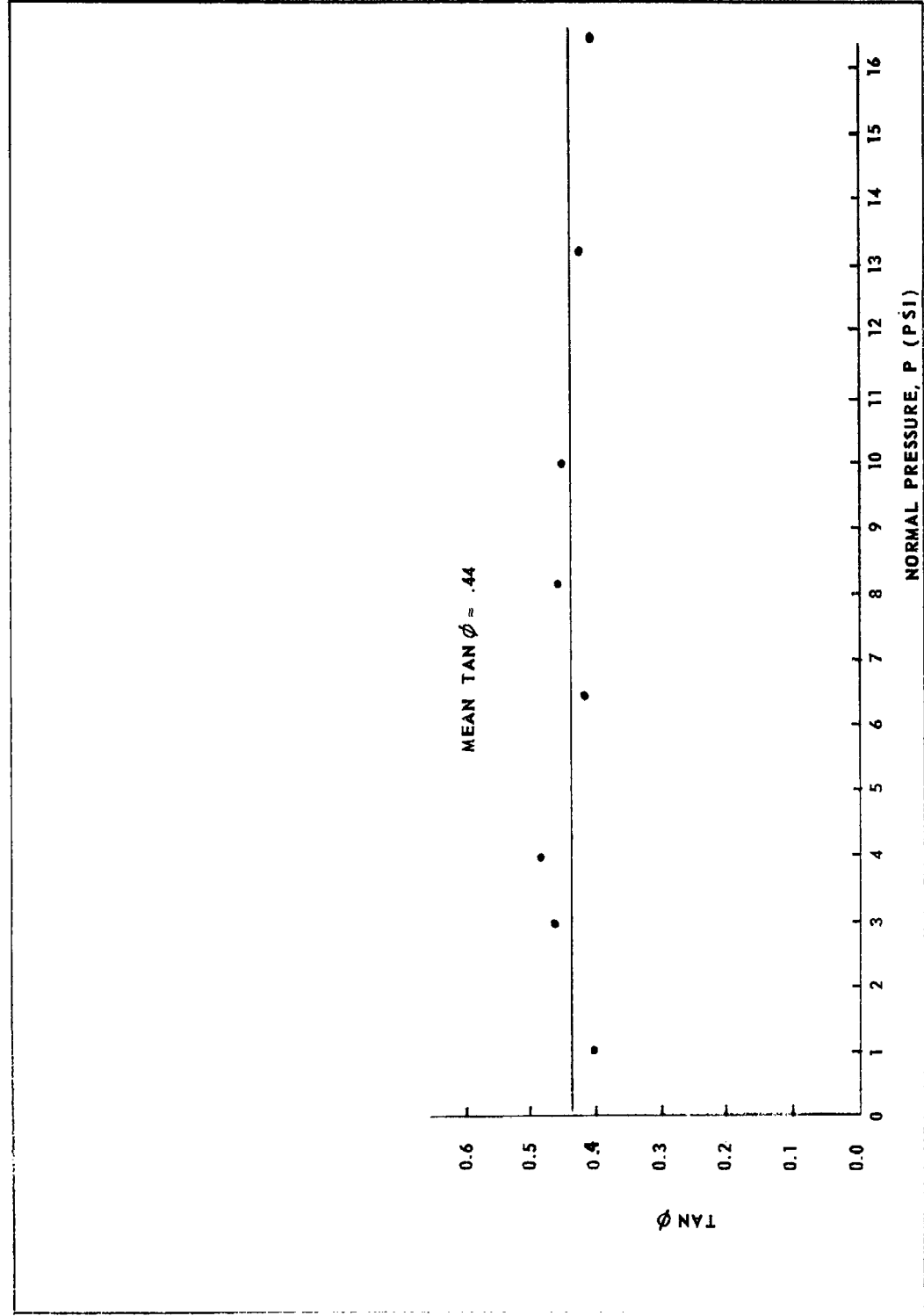


FIG. 16. EXPERIMENTAL VALUES OF TAN ϕ VERSUS NORMAL PRESSURE.

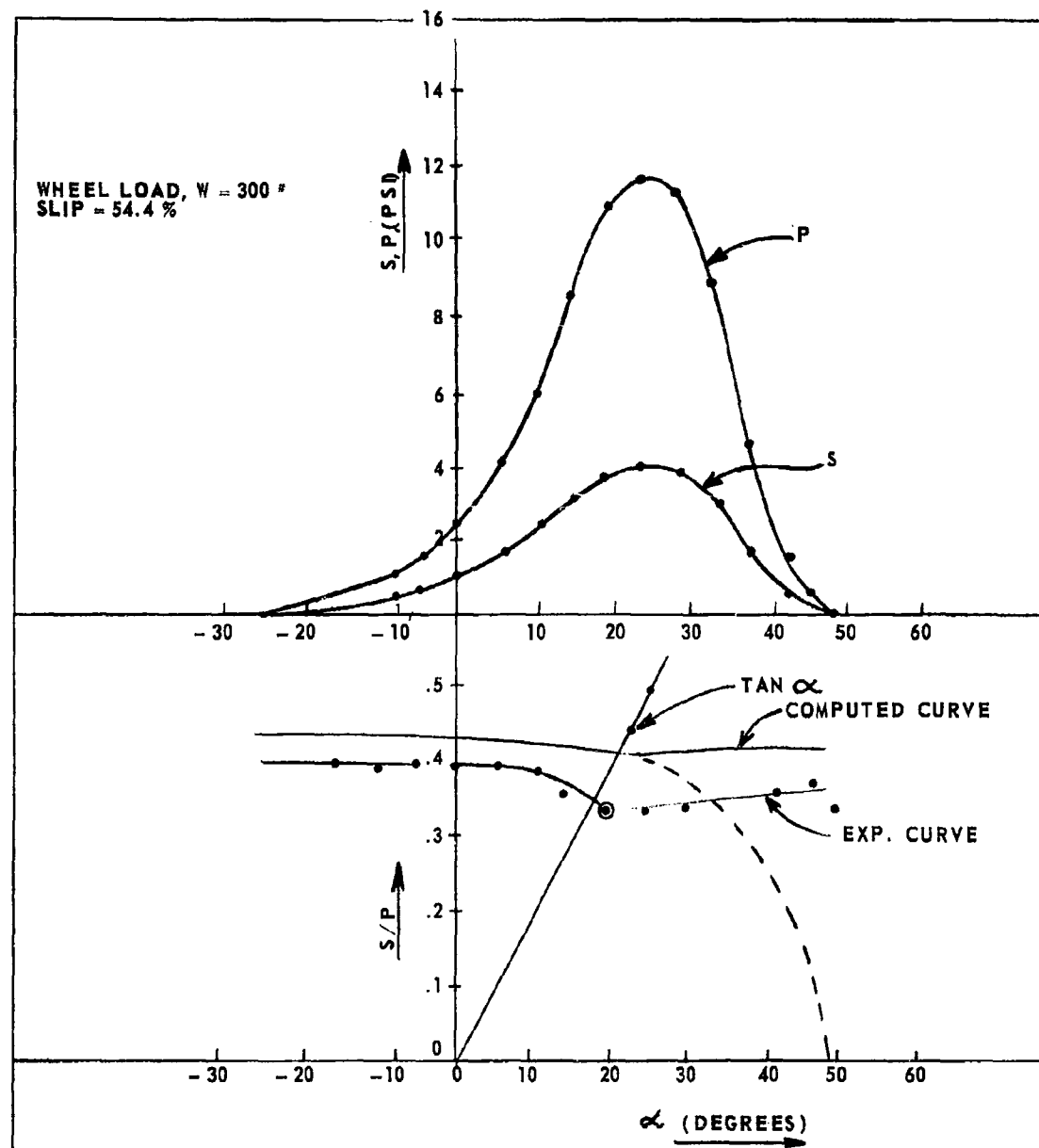


FIG. 17. SOIL STRESSES, SHEAR (S) AND NORMAL (P) UNDER A DRIVEN RIGID WHEEL IN SAND.

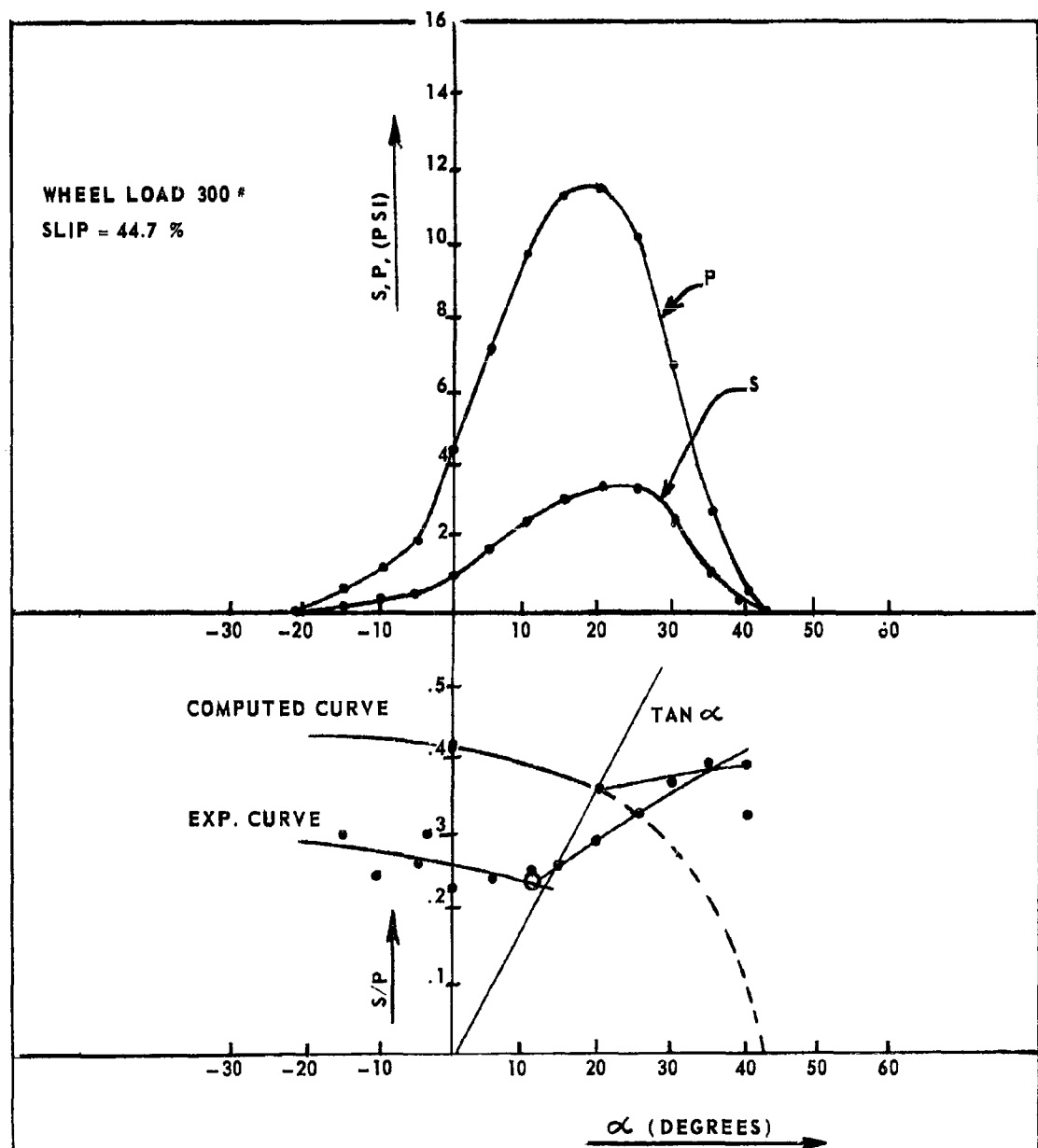


FIG. 18 SOIL STRESSES, SHEAR (S) AND NORMAL (P) UNDER A DRIVEN, RIGID WHEEL IN SAND.

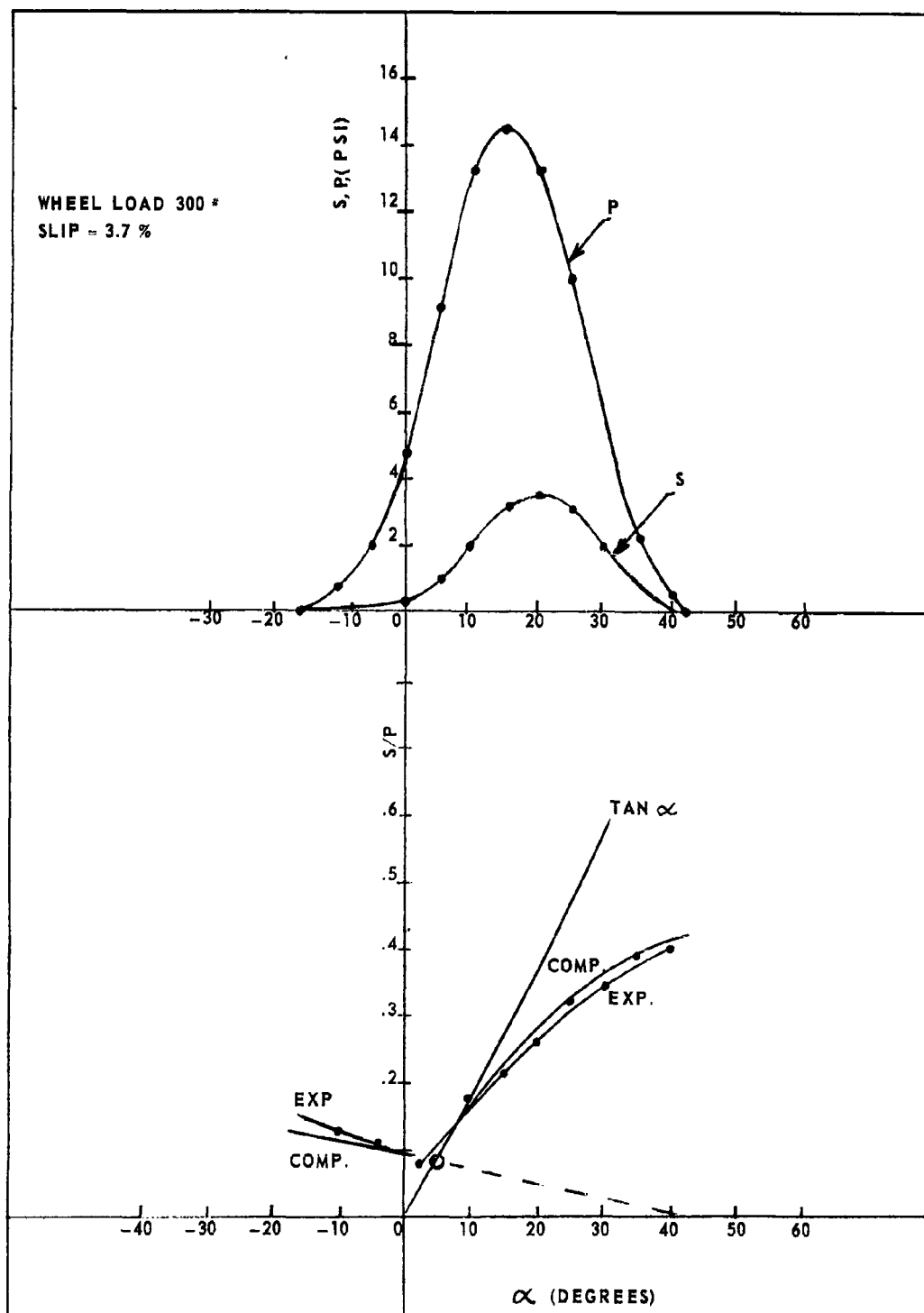


FIG. 19 SOIL STRESSES, SHEAR (S) AND NORMAL (P) UNDER A DRIVEN, RIGID WHEEL IN SAND.

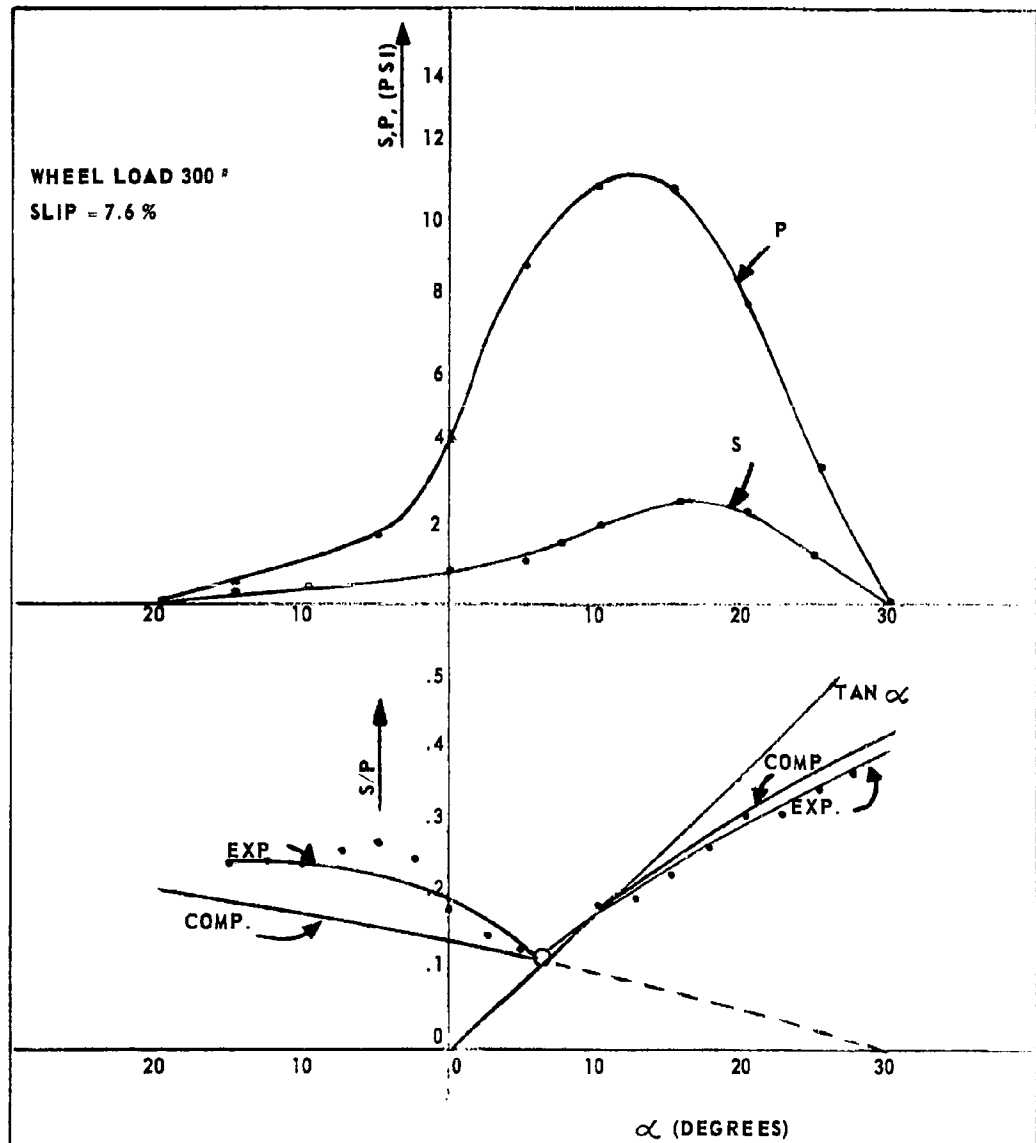


FIG. 20 SOIL STRESSES, SHEAR (S) AND NORMAL (P) UNDER A DRIVEN, RIGID, WHEEL IN SAND.

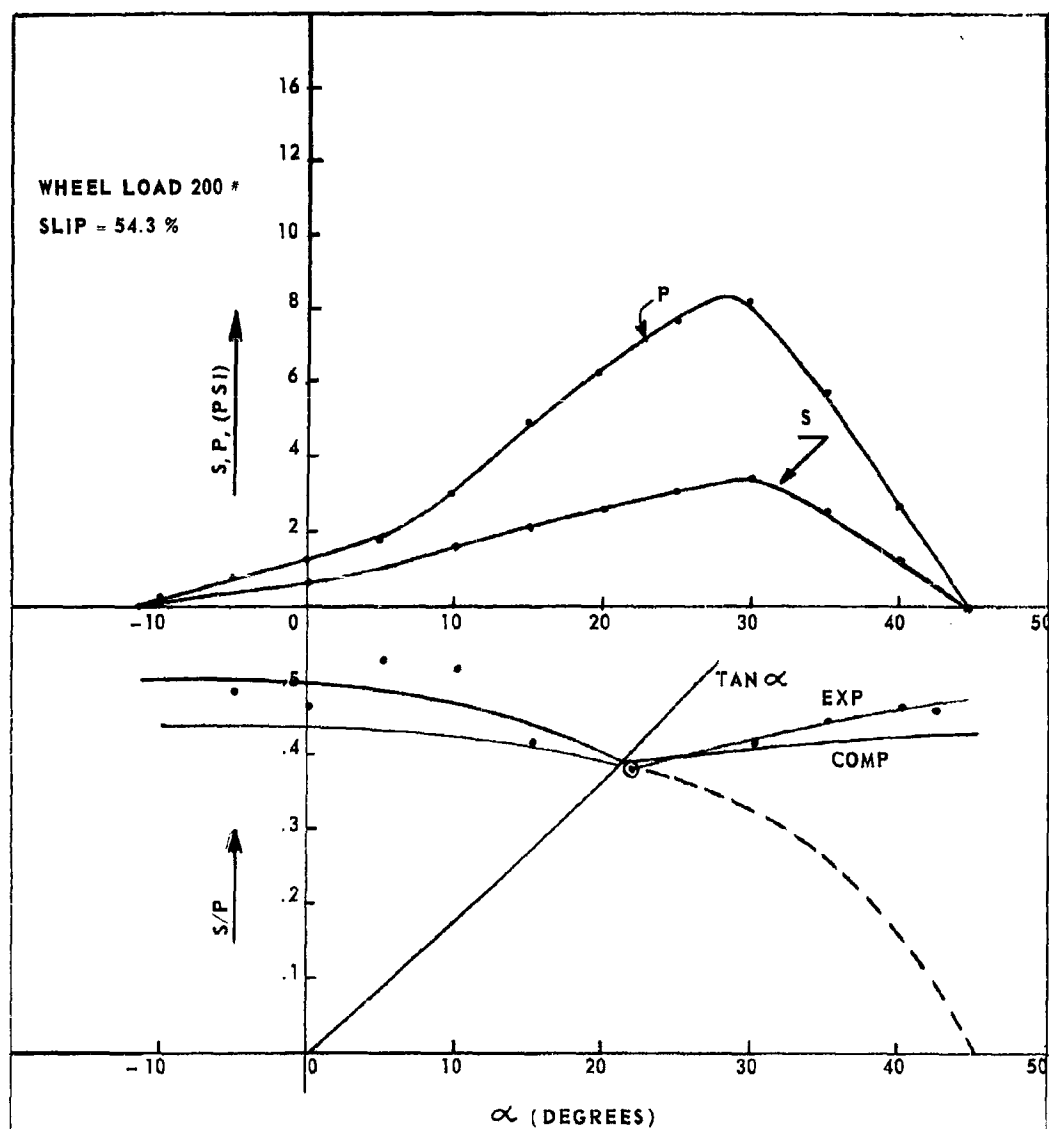


FIG. 21 SOIL STRESSES, SHEAR (S) AND NORMAL (P) UNDER A DRIVEN, RIGID WHEEL IN SAND.

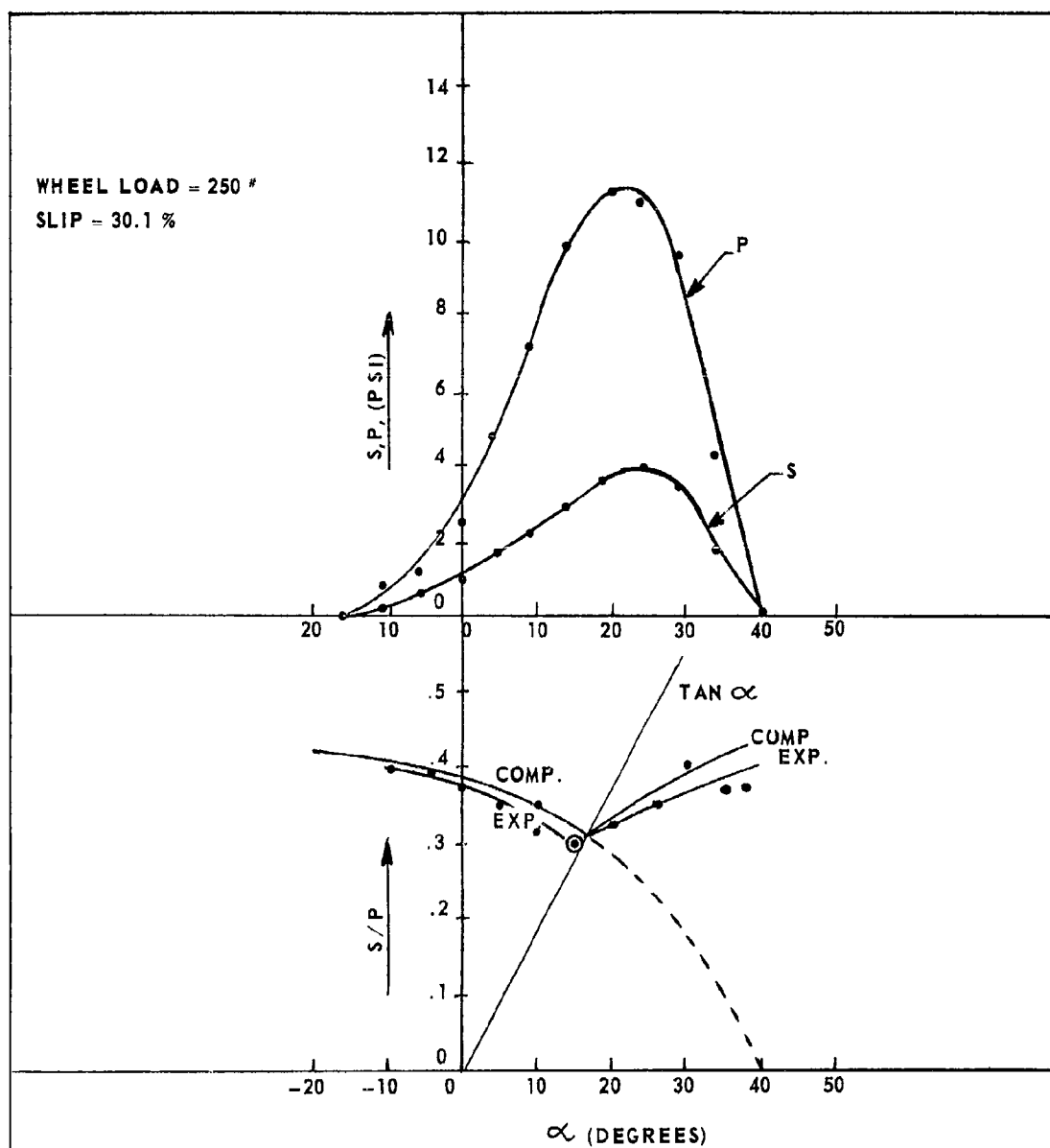


FIG. 22. SOIL STRESSES, SHEAR (S) AND NORMAL (P) UNDER A DRIVEN, RIGID WHEEL IN SAND.

WHEEL LOAD = 250 #
SLIP = 18.4 %

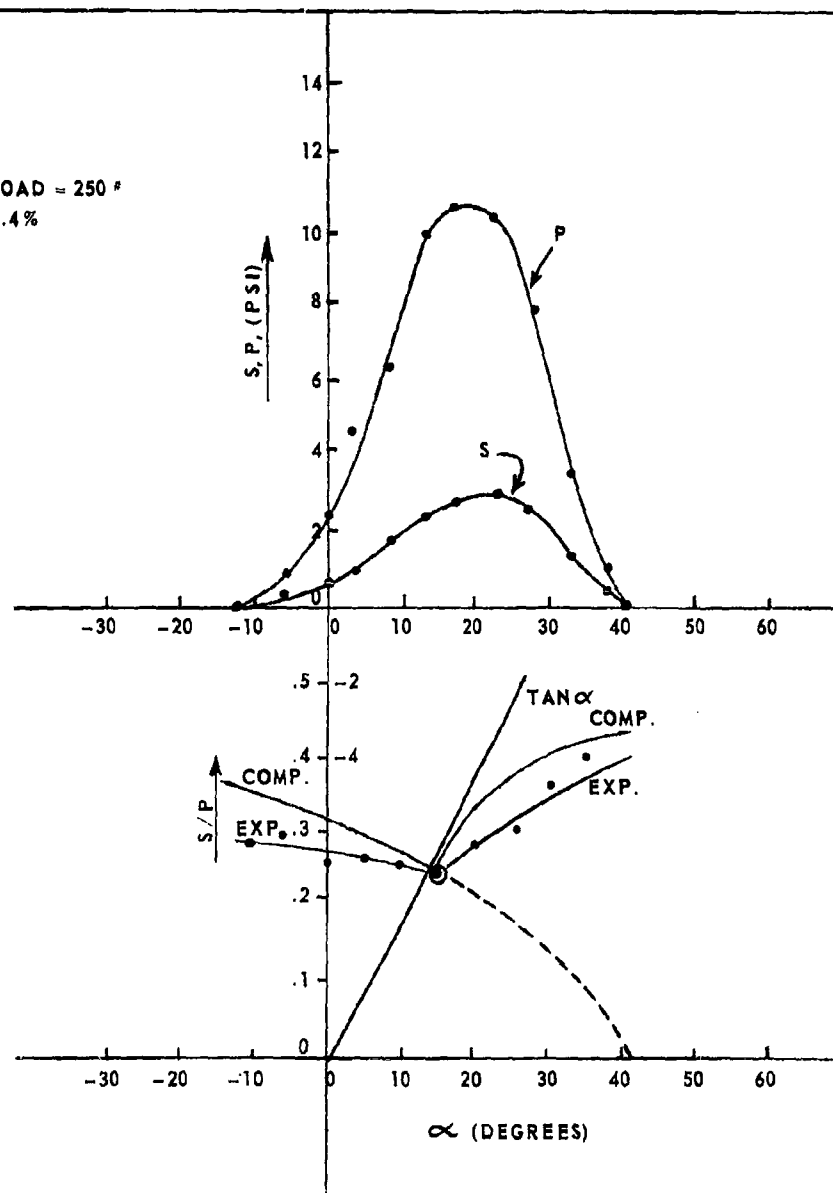


FIG. 23 SOIL STRESSES SHEAR (S) AND NORMAL (P) UNDER A DRIVEN, RIGID WHEEL IN SAND.

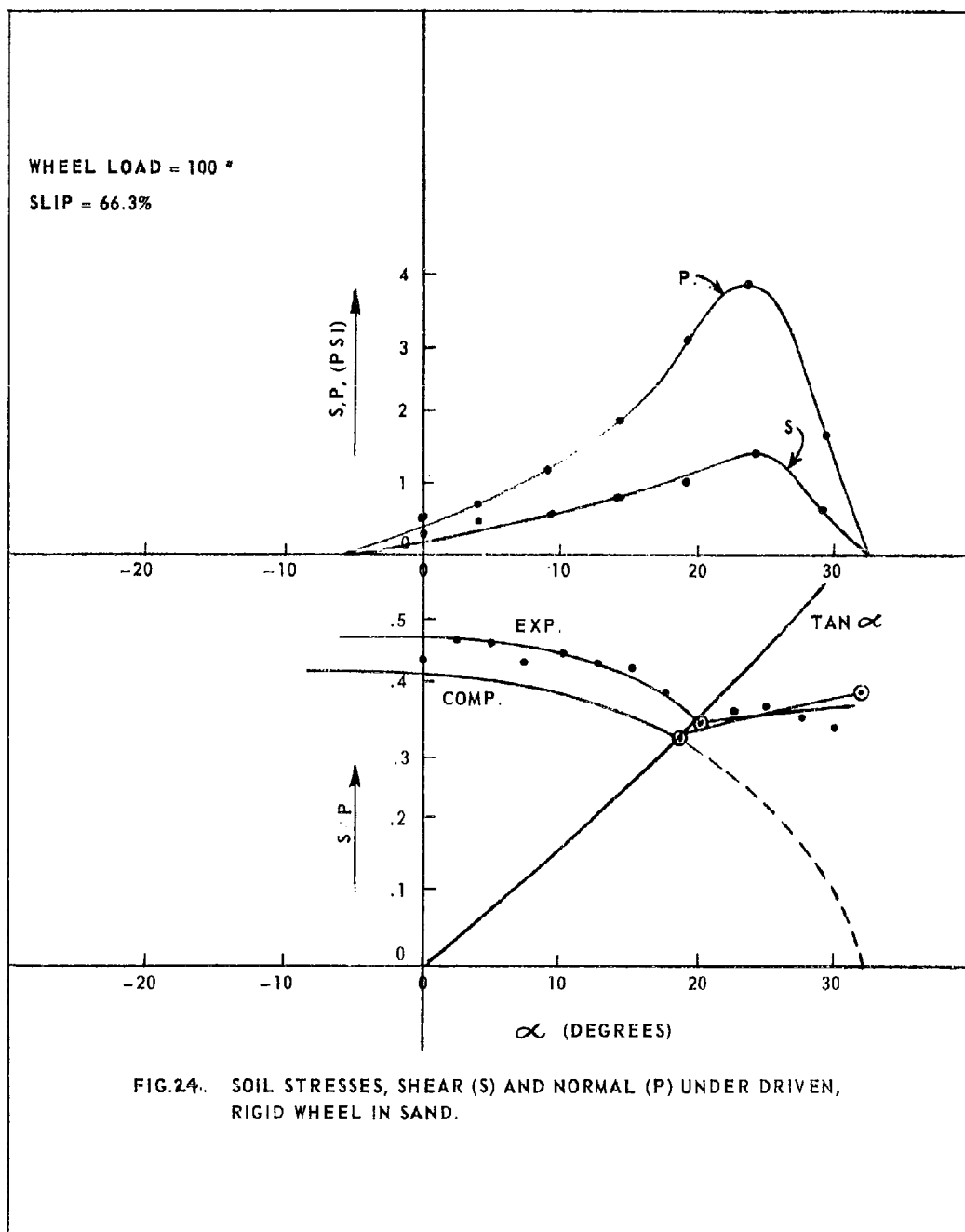
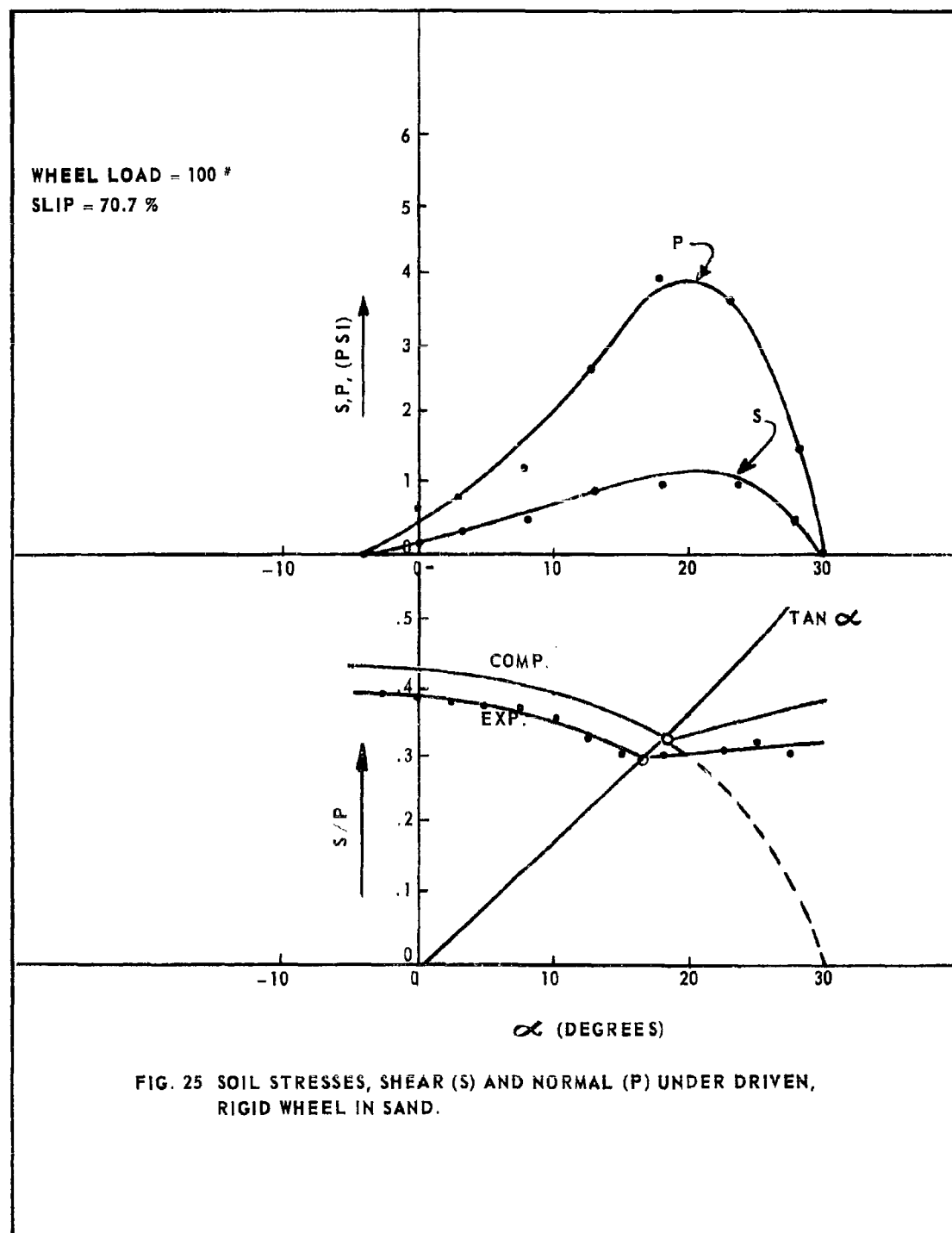
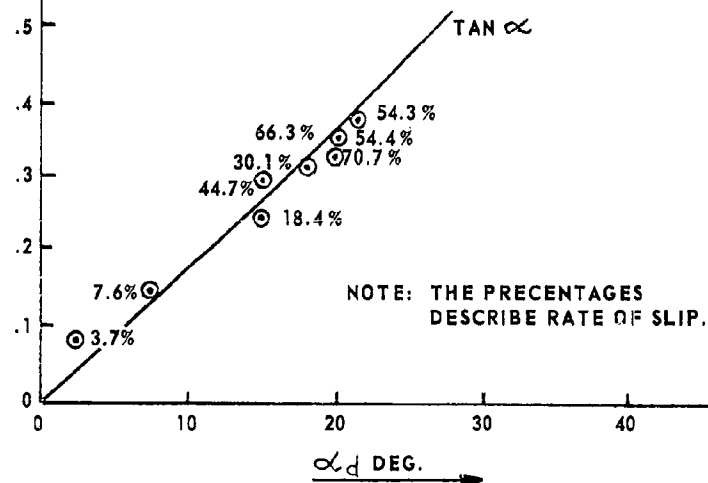


FIG.24. SOIL STRESSES, SHEAR (S) AND NORMAL (P) UNDER DRIVEN, RIGID WHEEL IN SAND.



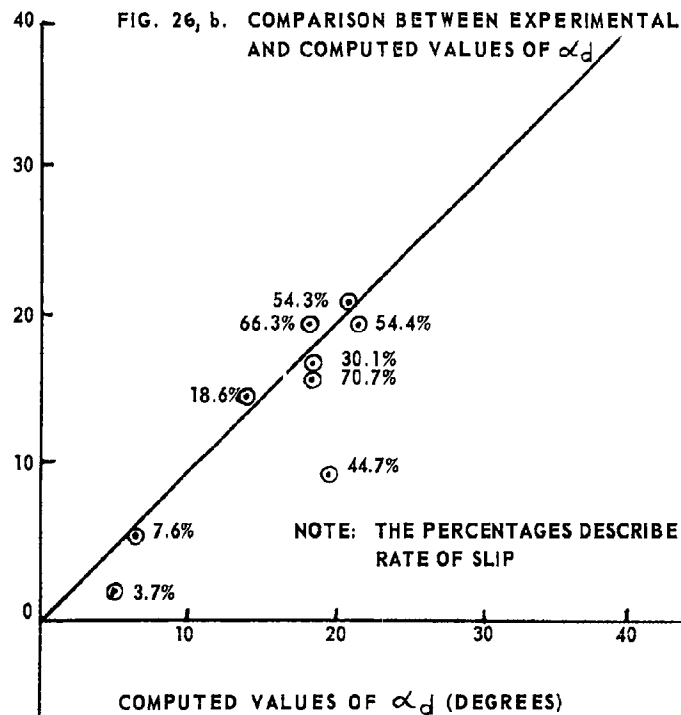
EXPERIMENTAL VALUES OF S/P at α_d

FIG. 26, a. SCATTER OF S/P FOR ANGLES α_d ALONG TAN α LINE.



EXPERIMENTAL VALUES OF α_d (DEGREES)

FIG. 26, b. COMPARISON BETWEEN EXPERIMENTAL AND COMPUTED VALUES OF α_d



WHEEL LOAD - 100 "
SKID - 37.7 %

EXP. $\alpha_r = 17^\circ$

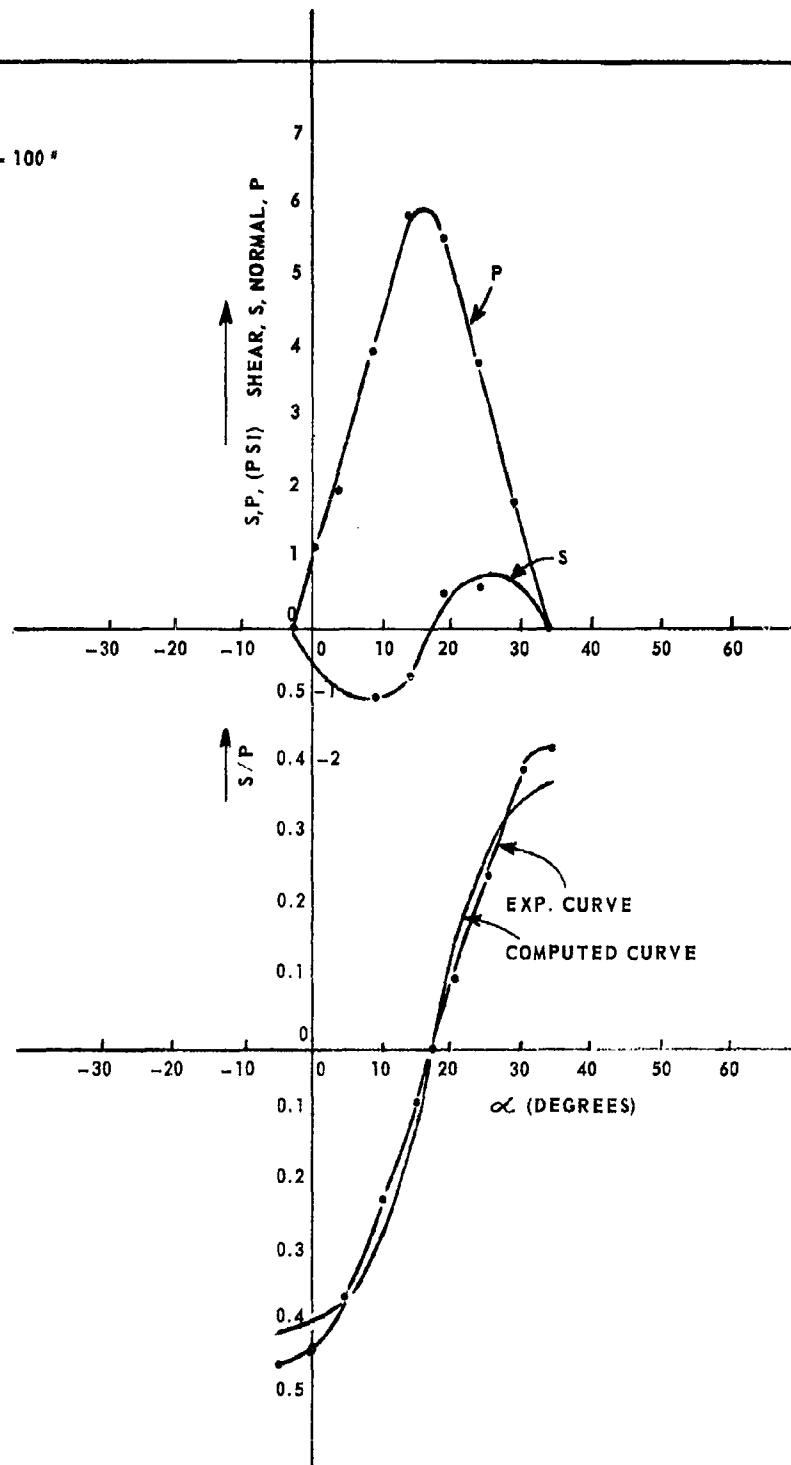


FIG. 27. SOIL STRESSES, SHEAR (S) AND NORMAL (P) UNDER A BRAKED, RIGID WHEEL IN SAND.

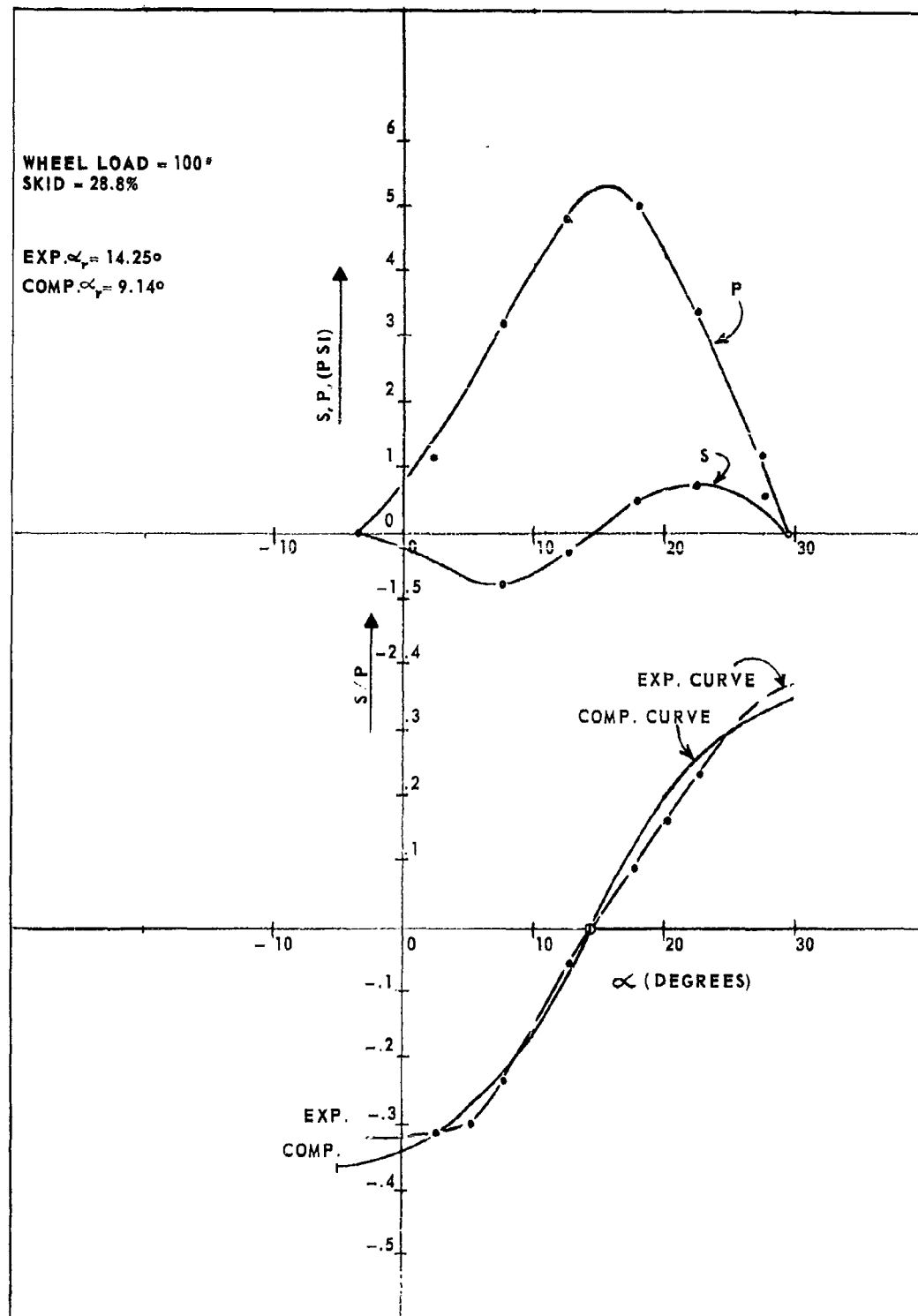


FIG. 28. SOIL STRESSES, SHEAR (S) AND NORMAL (P) UNDER A BRAKED, RIGID WHEEL IN SAND.

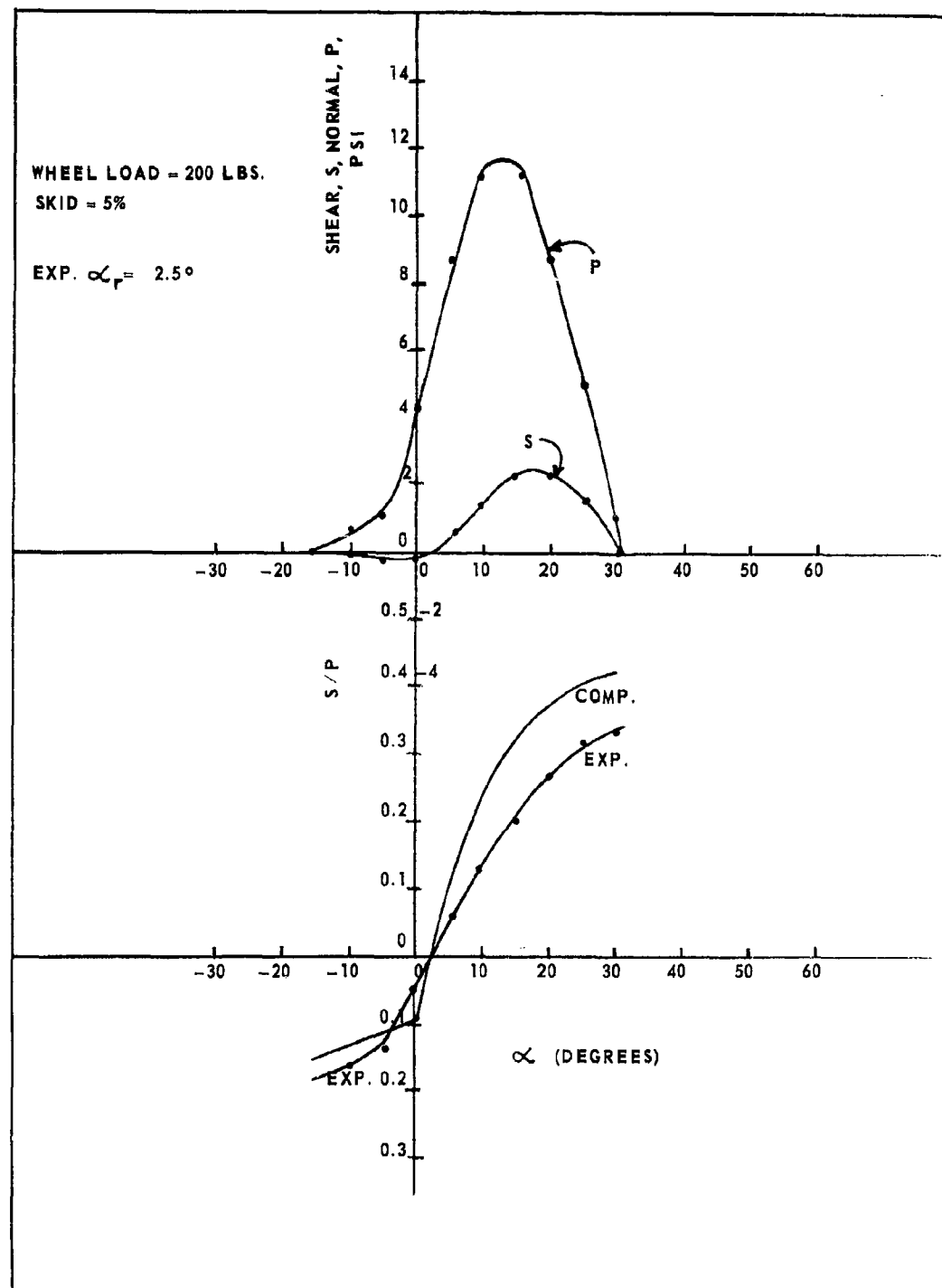


FIG. 29. STRESSES, SHEAR (S) AND NORMAL (P) UNDER A BRAKED, RIGID WHEEL IN SAND.

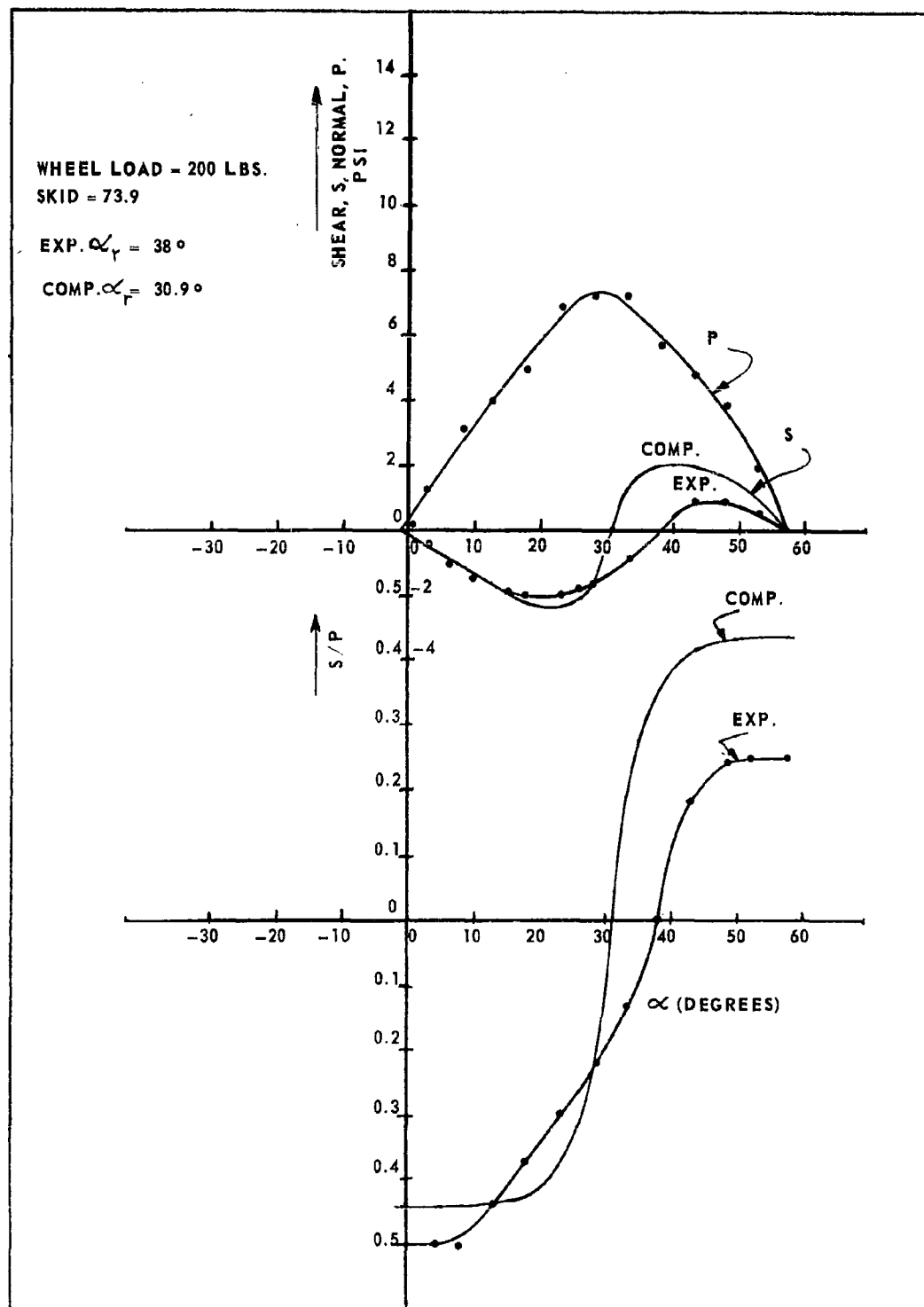


FIG. 30. SOIL STRESSES, SHEAR (S) AND NORMAL (P) UNDER A BRAKED, RIGID WHEEL IN SAND.

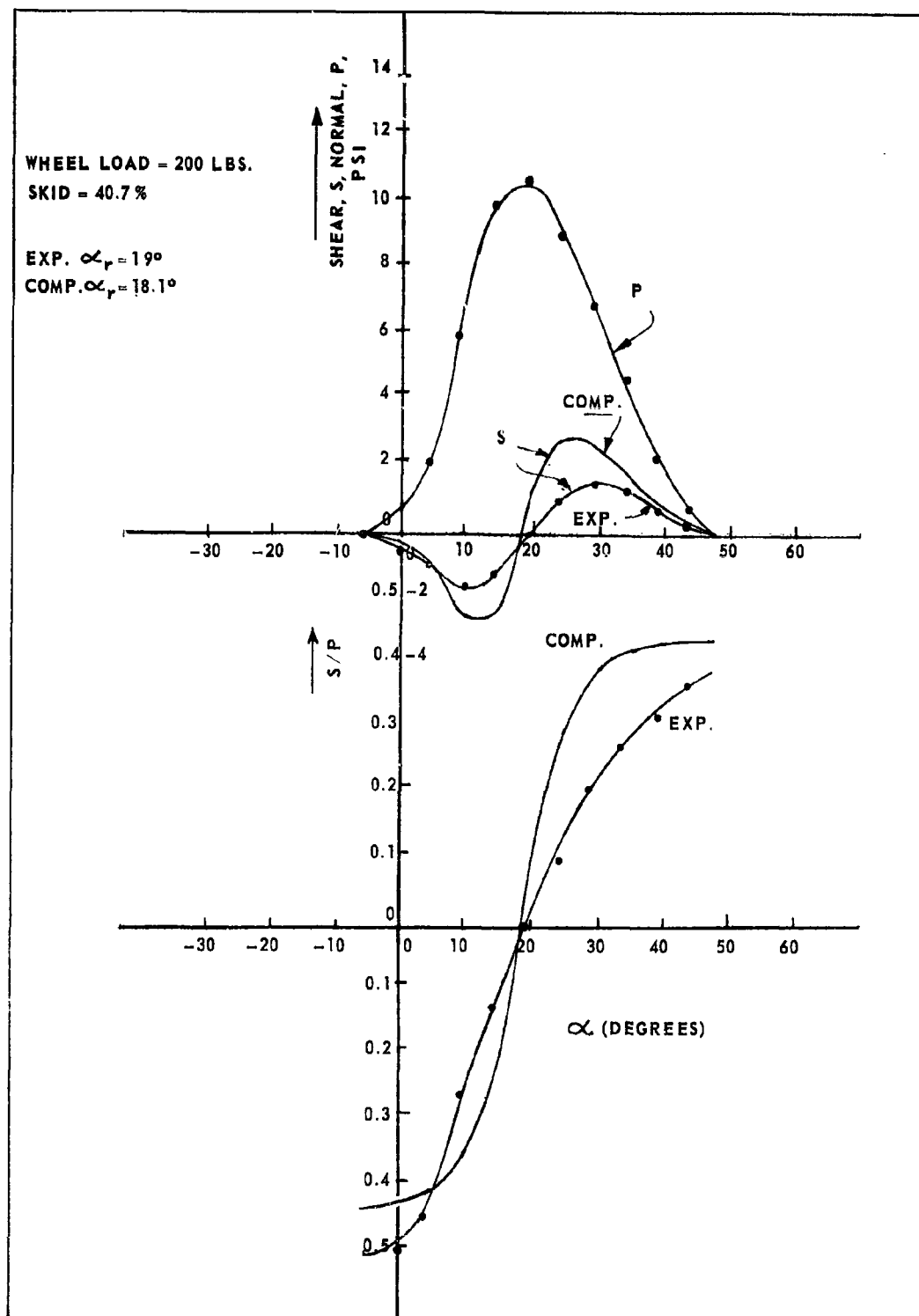


FIG. 31. SOIL STRESSES, SHEAR (S) AND NORMAL (P) UNDER A BRAKED, RIGID WHEEL IN SAND.

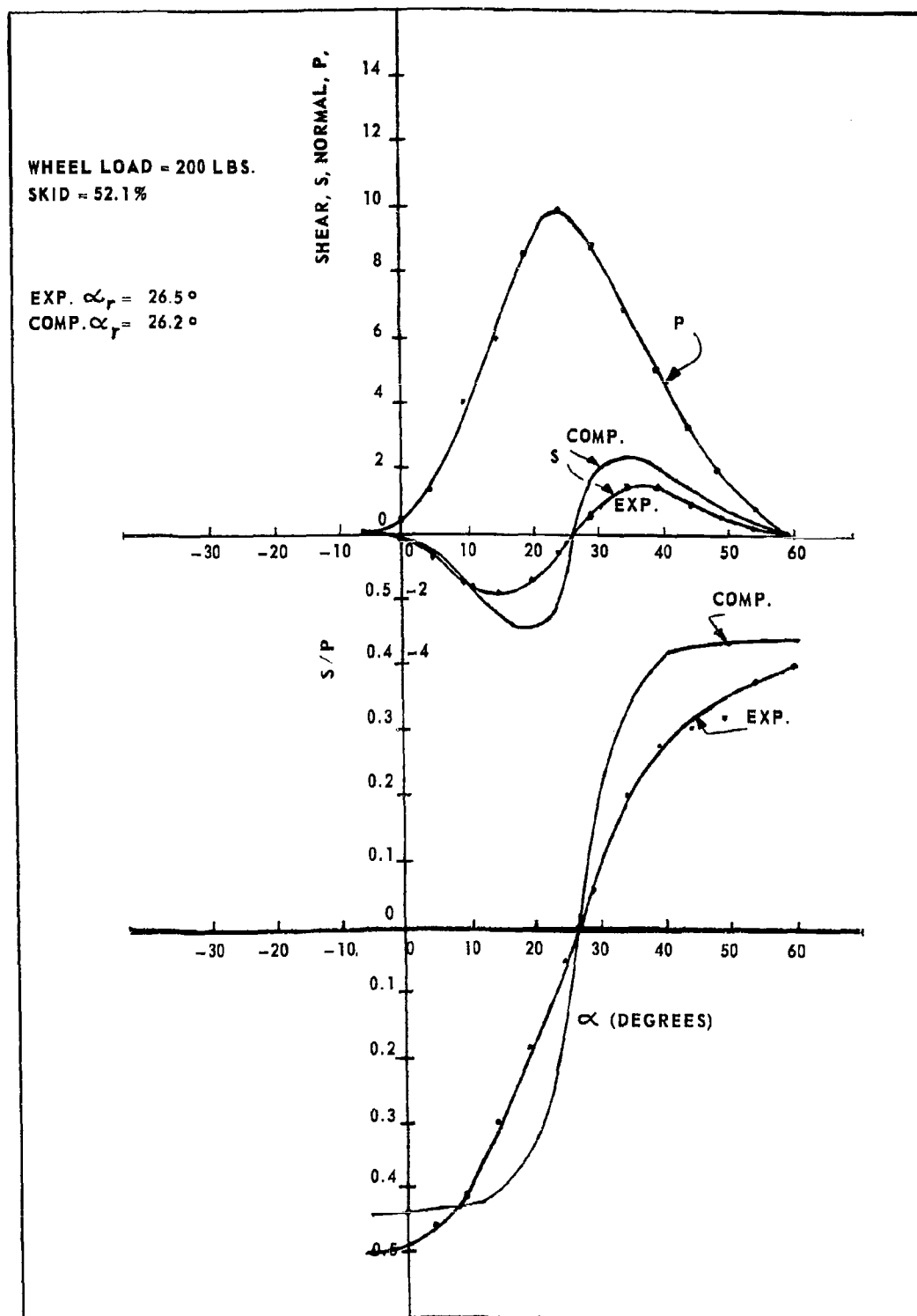


FIG. 32. SOIL STRESSES, SHEAR (S) AND NORMAL (P) UNDER A BRAKED, RIGID WHEEL IN SAND.

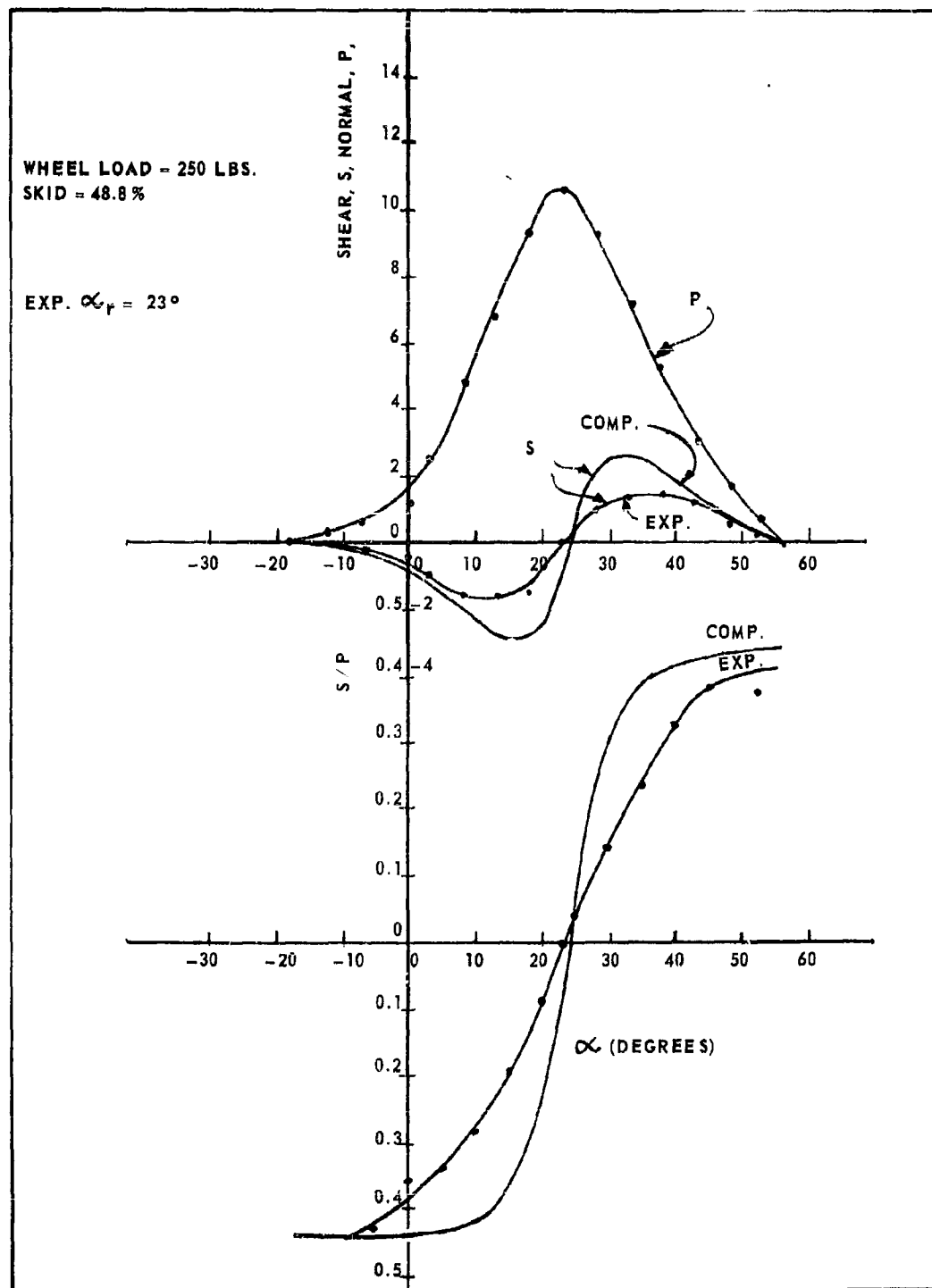


FIG. 33 SOIL STRESSES, SHEAR (S) AND NORMAL (P) UNDER A BRAKED, RIGID WHEEL IN SAND.

WHEEL LOAD = 250 LBS.
SKID = 14.5%

EXP. $\alpha_r = 9^\circ$

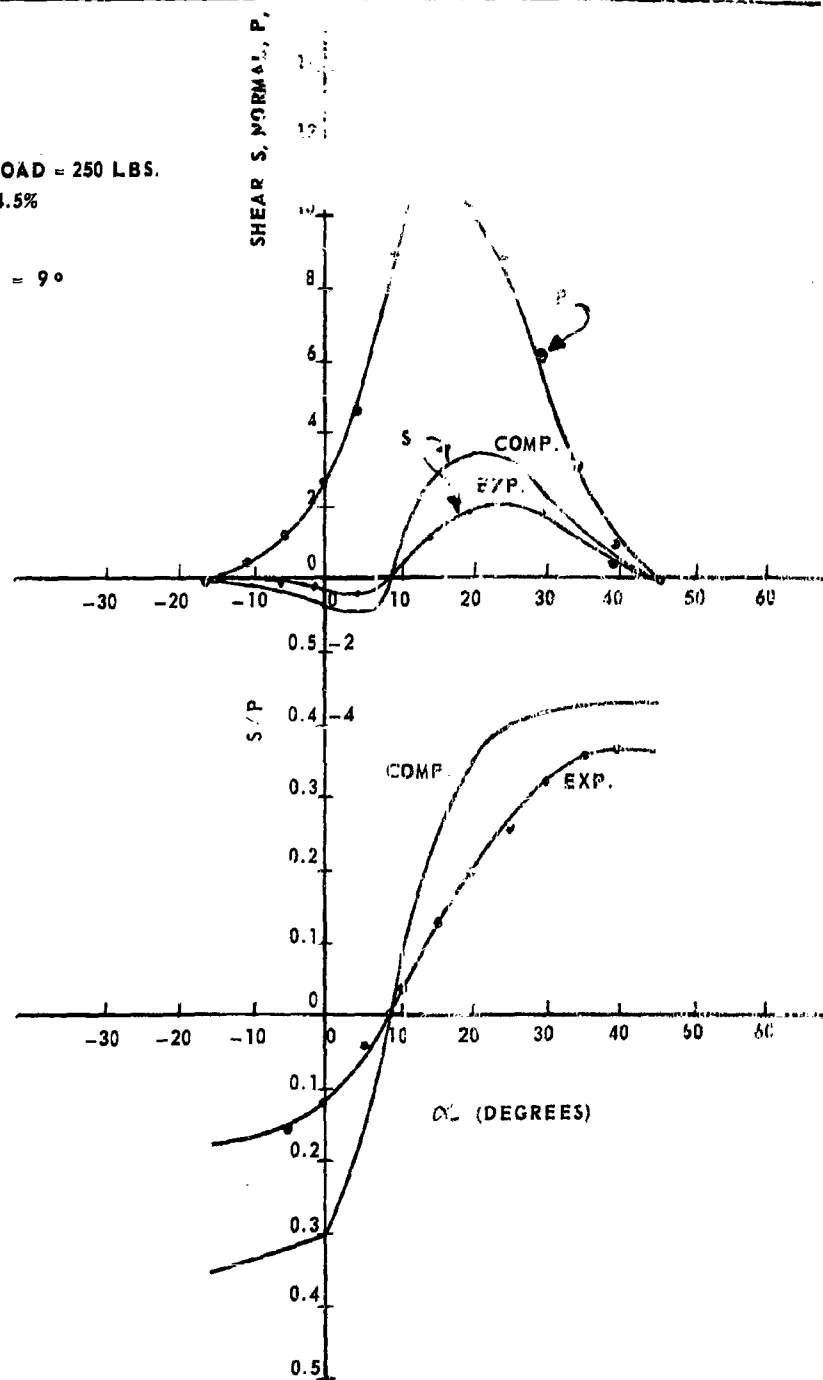


FIG. 34. SOIL STRESSES, SHEAR (S) AND NORMAL (P) UNDER A BRAKED, RIGID WHEEL IN SAND.

WHEEL LOAD = 300 LBS.

SKID = 57.8 %

EXP $\alpha_p = 31^\circ$

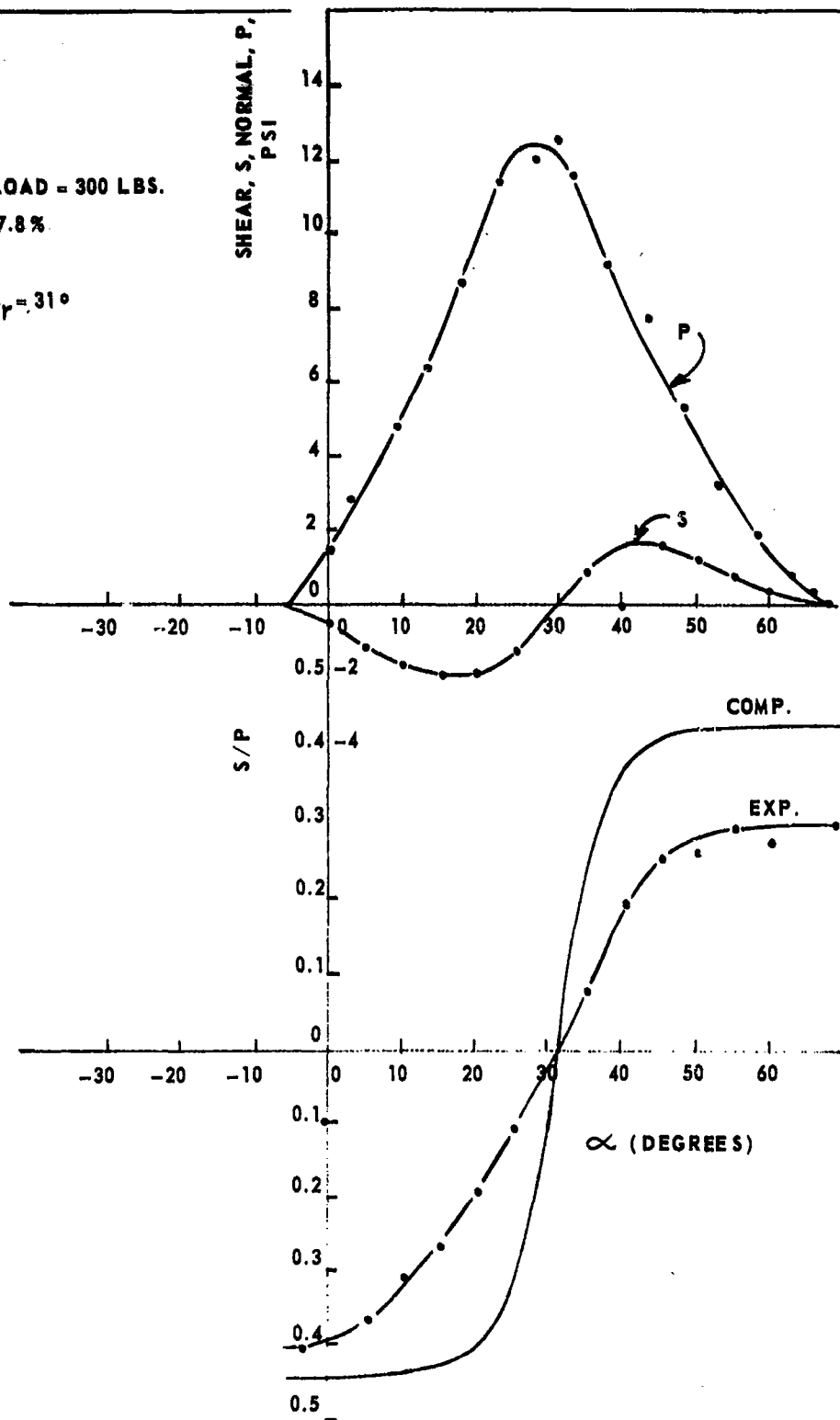


FIG. 35. SOIL STRESSES, SHEAR (S) AND NORMAL (P) UNDER A BRAKED, RIGID WHEEL IN SAND.

WHEEL LOAD = 300 LBS.
SKID = 40.0%

EXP. $\alpha_r = 22.5^\circ$

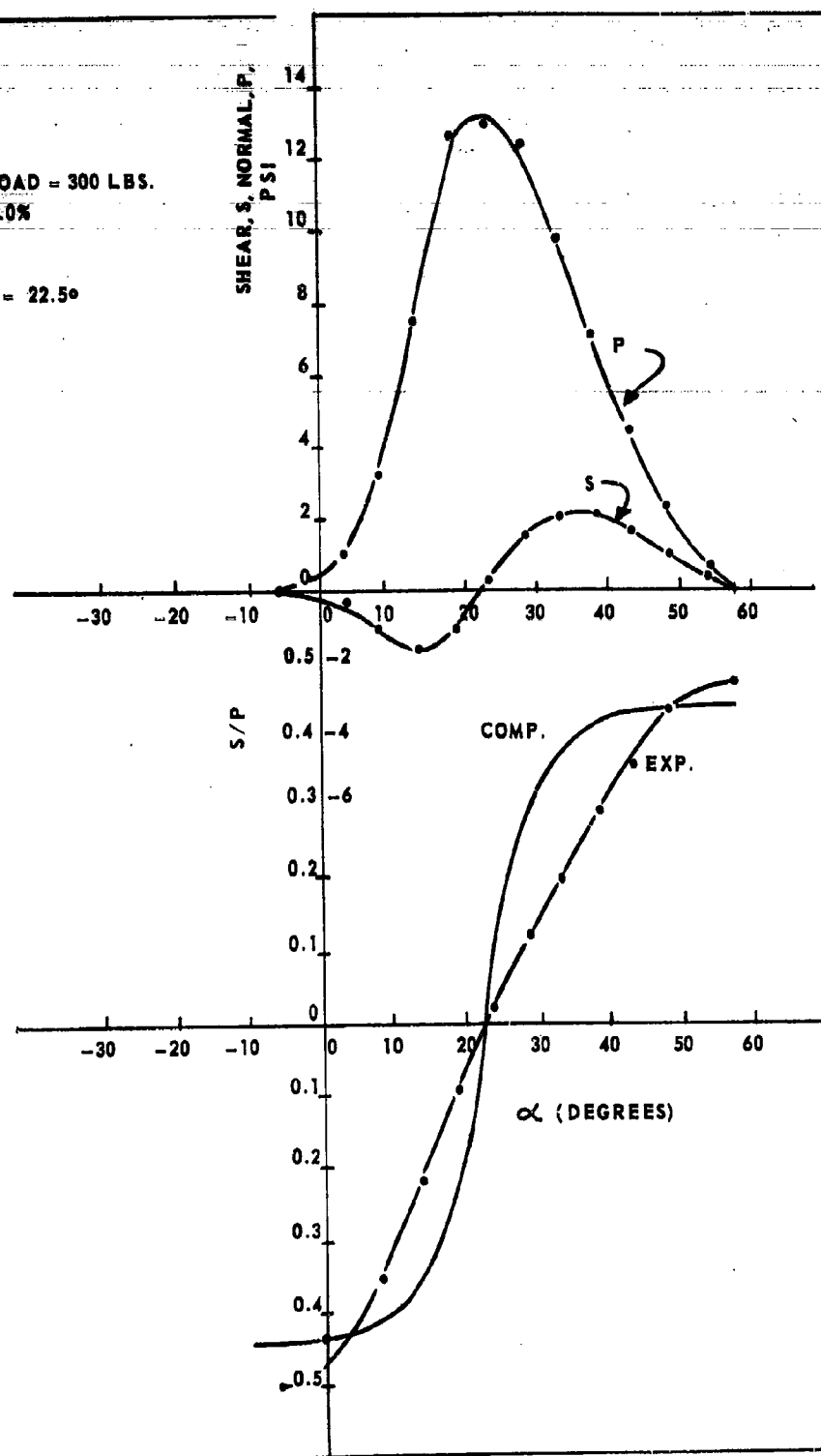


FIG. 36. SOIL STRESSES, SHEAR (S) AND NORMAL (P) UNDER A BRAKED, RIGID WHEEL.

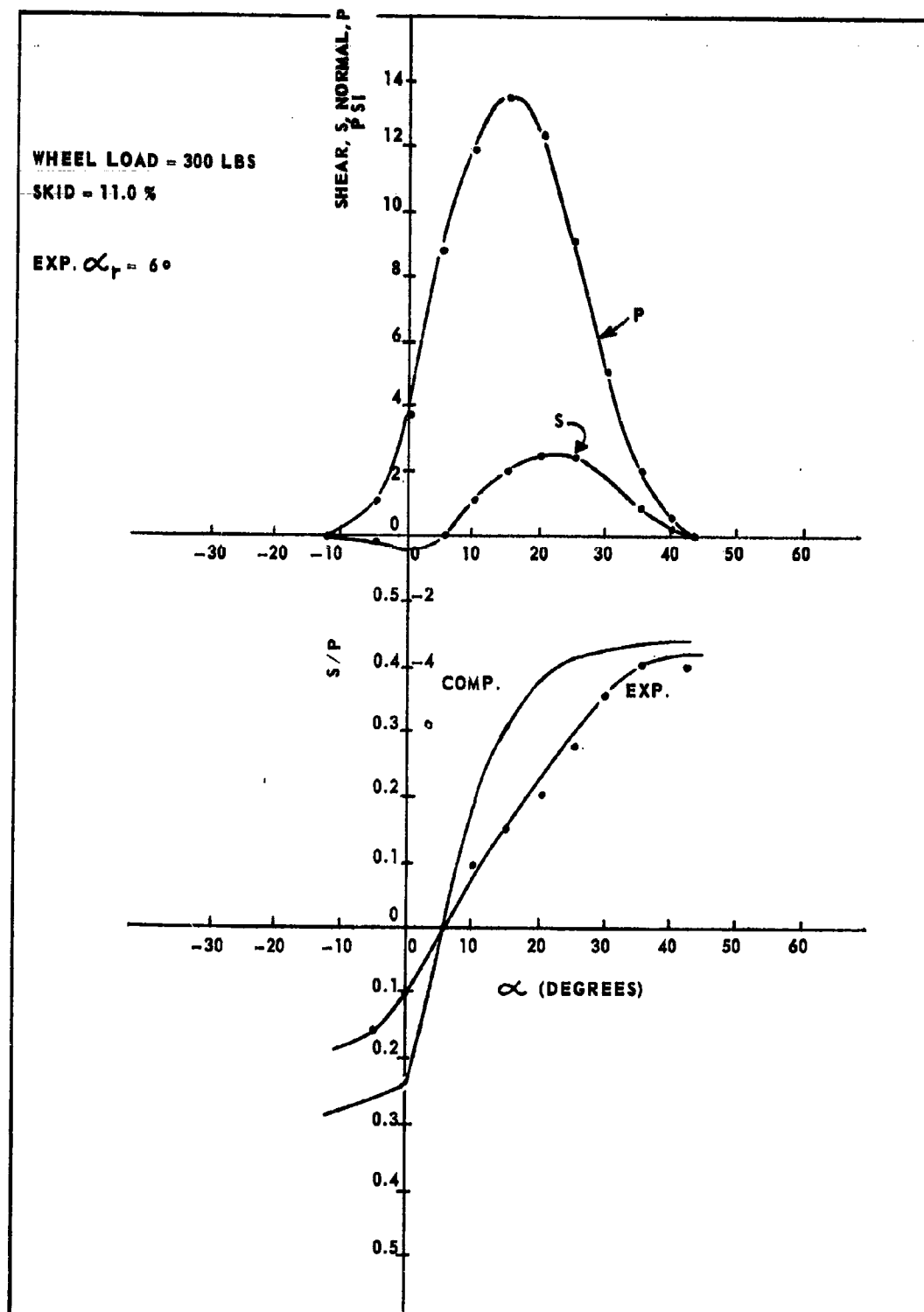
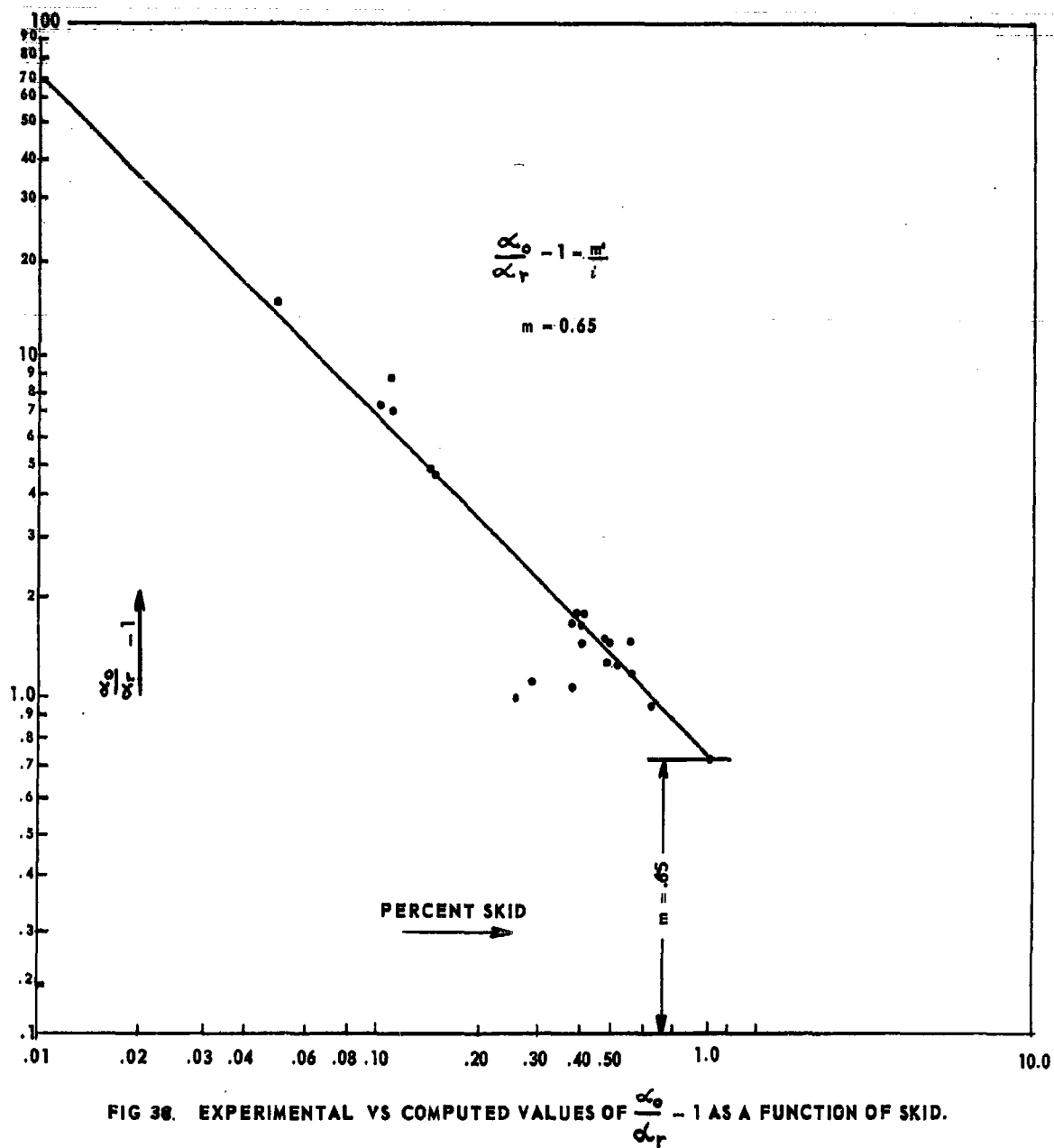


FIG. 37. SOIL STRESSES, SHEAR (S) AND NORMAL (P) UNDER A BRAKED, RIGID WHEEL.



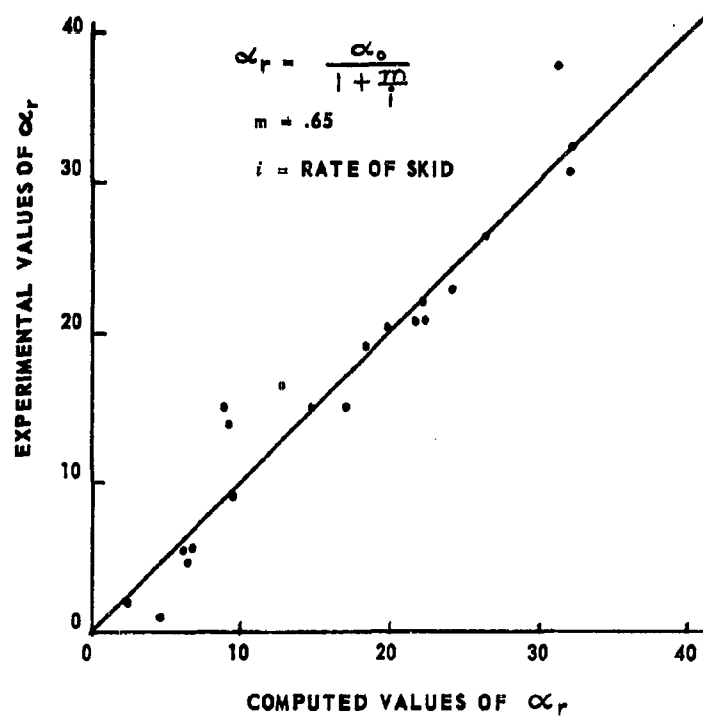


FIG. 39 A COMPARISON BETWEEN COMPUTED AND EXPERIMENTAL VALUES OF α_r , ANGLE OF SHEAR STRESSES REVERSING POINT ON BRAKED WHEELS.

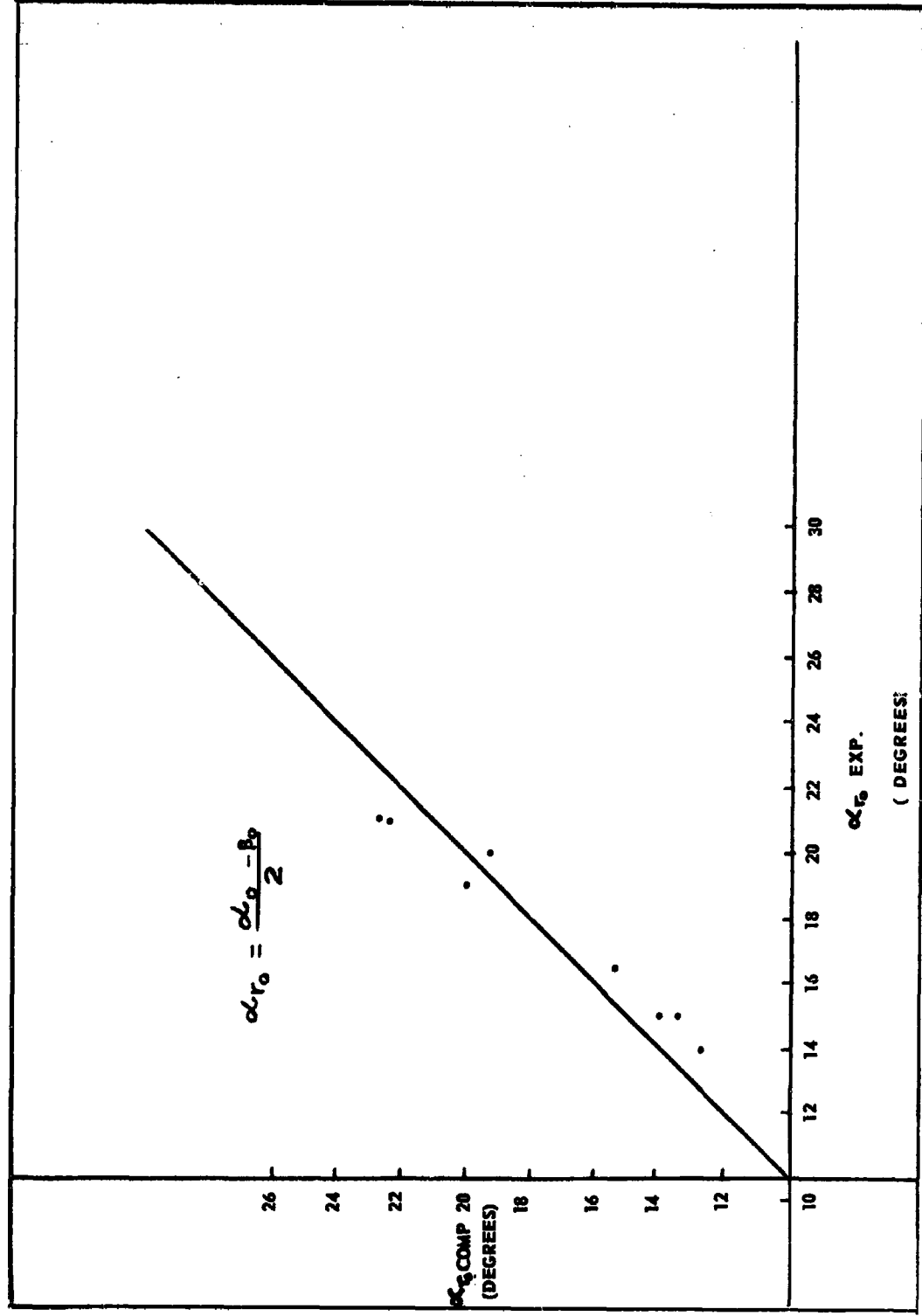


FIG. 40 COMPARISON OF COMPUTED VS EXPERIMENTAL VALUES OF α_{r_0}

<p>-UNCLASSIFIED-</p>	<p>AD</p>	<p>Accession No.</p>	<p>-UNCLASSIFIED-</p>
<p>THE SHEAR TO NORMAL STRESS RELATIONSHIP BETWEEN A RIGID WHEEL AND DRY SAND</p>	<p>Army Tank Automotive Center, Laboratories Division, Warren, Michigan</p>	<p>Report No. 3524, June 1964, 20 pp., 40 Figures - Unclassified Report</p>	<p>THE SHEAR TO NORMAL STRESS RELATIONSHIP BETWEEN A RIGID WHEEL AND DRY SAND</p>

Analytical expressions are formulated to describe the distribution of shear stresses which arise due to slip and soil flow.

The distribution of the shear and normal stresses along the wheel-soil interface is established as a function of slip. The stresses under a towed wheel are also described.

Actual measurements of the stresses by means of a special transducer embedded in the wheel are presented and compared to theoretical values. It is found that the agreement is satisfactory. It is concluded that further analysis of the available data will lead to a better understanding of the mechanics of tires operating off-the-road and to an improvement in wheeled vehicle prediction techniques.

[illegible]

analytical expressions are formulated to describe the distribution of shear stresses which arise due to slip and oil flow.

The distribution of the shear and normal stresses along the heel-soil interface is established as a function of slip. The stresses under a towed wheel are also described.

Actual measurements of the stresses by means of a special transducer embedded in the wheel are presented and compared with theoretical values. It is found that the agreement is satisfactory. It is concluded that further analysis of the available data will lead to a better understanding of the mechanics of tires operating off-the-road and to an improvement in wheeled vehicle prediction techniques.

AD	Accession No.	-UNCLASSIFIED-
Army Tank Automotive Center, Laboratories Division, Warren, Michigan		
THE SHEAR TO NORMAL STRESS RELATIONSHIP BETWEEN A RIGID WHEEL AND DRY SAND - Lt. Col. Aharon D. Sela Report No. 3524, June 1964, 20 pp., 40 Figures - Unclassified Report		THE SHEAR TO NORMAL STRESS RELATIONSHIP BETWEEN A RIGID WHEEL AND DRY SAND
Analytical expressions are formulated to describe the distribution of shear stresses which arise due to slip and soil flow.		

Analytical expressions are formulated to describe the distribution of shear stresses which arise due to slip and soil flow.

The distribution of the shear and normal stresses along the wheel-soil interface is established as a function of slip. The stresses under a towed wheel are also described.

Actual measurements of the stresses by means of a special transducer embedded in the wheel are presented and compared to theoretical values. It is found that the agreement is satisfactory. It is concluded that further analysis of the available data will lead to a better understanding of the mechanics of tires operating off-the-road and to an improvement in wheeled vehicle prediction techniques.

AD	Accession No.	- UNCLASSIFIED-
Army Tank Automotive Center, Laboratories Division, Warren, Michigan		
THE SHEAR TO NORMAL STRESS RELATIONSHIP BETWEEN A RIGID WHEEL AND DRY SAND - Lt. Col. Aharon D. Sela		
Report No. 8524, June 1964. 20 pp.. 40 Figures - Unclassified Report		
Analytical expressions are formulated to describe the distribution of shear stresses which arise due to slip and soil flow		

Analytical expressions are formulated to describe the distribution of shear stresses which arise due to slip and soil flow.

The distribution of the shear and normal stresses along the wheel-soil interface is established as a function of slip. The stresses under a towed wheel are also described.

Actual measurements of the stresses by means of a special transducer embedded in the wheel are presented and compared to theoretical values. It is found that the agreement is satisfactory. It is concluded that further analysis of the available data will lead to a better understanding of the mechanics of tires operating off-the-road and to an improvement in wheeled vehicle prediction techniques.

AD Accession No.
Army Tank Automotive Center, Laboratories Division,
Warren, Michigan
THE SHEAR TO NORMAL STRESS RELATIONSHIP BETWEEN A RIGID
WHEEL AND DRY SAND - Lt. Col. Aharon D. Seia
Report No. 8504 June 1964, 20 pp., 40 Figures -
Unclassified Report

ANALYTICAL EXPRESSIONS ARE FORMULATED TO DESCRIBE THE
DISTRIBUTION OF SHEAR STRESSES WHICH ARISE DUE TO SLIP AND
SOIL FLOW.

THE DISTRIBUTION OF THE SHEAR AND NORMAL STRESSES ALONG THE
WHEEL-SOIL INTERFACE IS ESTABLISHED AS A FUNCTION OF SLIP.
THE STRESSES UNDER A TOWED WHEEL ARE ALSO DESCRIBED.

ACTUAL MEASUREMENTS OF THE STRESSES BY MEANS OF A SPECIAL
TRANSDUCER EMBEDDED IN THE WHEEL ARE PRESENTED AND COMPARED
TO THEORETICAL VALUES. IT IS FOUND THAT THE AGREEMENT IS
SATISFACTORY. IT IS CONCLUDED THAT FURTHER ANALYSIS OF THE
AVAILABLE DATA WILL LEAD TO A BETTER UNDERSTANDING OF THE
MECHANICS OF TIRES OPERATING OFF-THE-ROAD AND TO AN
IMPROVEMENT IN WHEELED VEHICLE PREDICTION TECHNIQUES.

UNCLASSIFIED

AD	Accession No.
Army Tank Automotive Center, Warren, Michigan	
THE SHEAR TO NORMAL STRESS RELATIONSHIP BETWEEN A RIGID WHEEL AND DRY SAND - Lt. Col. Aharon D. Sela	
Report No. 3524, June 1964, 20 pp., 40 Figures -	
Unclassified Report	
Analytical expressions are formulated to describe the distribution of shear stresses which arise due to slip and soil flow.	
The distribution of the shear and normal stresses along the wheel-soil interface is established as a function of slip. The stresses under a towed wheel are also described.	
Actual measurements of the stresses by means of a special transducer embedded in the wheel are presented and compared to theoretical values. It is found that the agreement is satisfactory. It is concluded that further analysis of the available data will lead to a better understanding of the mechanics of tires operating off-the-road and to an improvement in wheeled vehicle prediction techniques.	

AD Accession No. Army Tank Automotive Center, Laboratories Division.
Warren, Michigan
THE SHEAR TO NORMAL STRESS RELATIONSHIP BETWEEN A RIGID WHEEL AND DRY SAND - Lt. Col. Aharon D. Sela
Report No. 524, June 1964. 20 pp., 40 Figures -
Unclassified Report

Analytical expressions are formulated to describe the distribution of shear stresses which arise due to slip and soil flow.

The distribution of the shear and normal stresses along the wheel-soil interface is established as a function of slip. The stresses under a towed wheel are also described.

Actual measurements of the stresses by means of a special transducer embedded in the wheel are presented and compared to theoretical values. It is found that the agreement is satisfactory. It is concluded that further analysis of the available data will lead to a better understanding of the mechanics of tires operating off-the-road and to an improvement in wheeled vehicle prediction techniques.

AC Accession No. _____
Army Tank Automotive Center, Laboratories Division,
Warren, Michigan

THE SHEAR TO NORMAL STRESS RELATIONSHIP BETWEEN A RIGID WHEEL AND DRY SAND - Lt. Col. Aharon D. Sola
Report No. 5523, June 1964, 20 pp., 40 Figures -
Unclassified Report

Analytical expressions are formulated to describe the distribution of shear stresses which arise due to slip and soil flow.

The distribution of the shear and normal stresses along the wheel-soil interface is established as a function of slip. The stresses under a towed wheel are also described.

Actual measurements of the stresses by means of a special transducer embedded in the wheel are presented and compared to theoretical values. It is found that the agreement is satisfactory. It is concluded that further analysis of the available data will lead to a better understanding of the mechanics of tires operating off-the-road and to an improvement in wheeled vehicle prediction techniques.

- UNCLASSIFIED -

THE SHEAR TO
NORMAL STRESS
RELATIONSHIP
BETWEEN A RIGID
WHEEL AND DRY
SAND

UNCLASSIFIED

UNCLASSIFIED